5.14 True Polar Wander: Linking Deep and Shallow Geodynamics to Hydro- and Bio-Spheric Hypotheses

T. D. Raub, Yale University, New Haven, CT, USA

J. L. Kirschvink, California Institute of Technology, Pasadena, CA, USA

D. A. D. Evans, Yale University, New Haven, CT, USA

5.14.1 Planetary Moment of Inertia and the Spin-Axis

Planets, as quasi-rigid, self-gravitating bodies in free space, must spin about the axis of their principal moment of inertia (Gold, 1955). Net angular momentum (the **L** vector), a conserved quantity in the absence of external torques, is related to the spin vector ($\boldsymbol{\omega}$) by the moment of inertia tensor (**I**) such that $\mathbf{L} = \mathbf{I}\boldsymbol{\omega}$. It is well known that the movement of masses within or on the solid Earth, such as sinking slabs of oceanic lithosphere, rising or erupting plume heads, or growing or waning ice sheets, can alter components of that inertial tensor and induce compensating changes in the $\boldsymbol{\omega}$ vector so that **L** is conserved. Observable mass redistributions caused by postglacial isostatic readjustment, by earthquakes, and even by weather systems cause detectible $\boldsymbol{\omega}$ changes, manifested as shifts in the geographic location of Earth's daily rotation axis and/or by fluctuations in the spin rate ('length of day' anomalies). Generally, such shift of the geographic rotation pole is called true polar wander (TPW).

Because its mantle and lithosphere are viscoelastic, Earth's daily spin distorts its shape slightly from that of a perfect sphere, producing an equatorial bulge of about 1 part in 300, or an excess equatorial radius of ~20 km relative to its polar radius. Variations in Earth's spin vector ($\boldsymbol{\omega}$) will cause this hydrostatic bulge to shift in response, with a characteristic timescale of ~10^5 years, governed by the relaxation time of the mantle to long-wavelength loads (Ranalli, 1995; Steinberger and Oconnell, 1997).

Goldreich and Toomre (1969) demonstrated that this hydrostatic bulge only exerts a stabilizing influence on the orientation of the planetary spin vector on timescales < ~10^5 years, with little or no influence on the bulk solid Earth over longer timescales (see also Richards *et al.*, 1997; Steinberger and Oconnell, 1997; Steinberger and O'Connell, 2002). For the purposes of this discussion, only the nonhydrostatic component of Earth's inertial tensor is geologically important, and inertial perturbations of sufficient scale should induce TPW in a sense that moves a new principal inertial axis ($\mathbf{I}_{max}$) back toward the average rotation vector, $\boldsymbol{\omega}$.

5.14.2 Apparent Polar Wander (APW) = Plate motion + TPW

5.14.2.1 Different Information in Different Reference Frames

For mid-Mesozoic and younger time, seafloor magnetic lineations permit accurate paleogeographic reconstructions of continents separated by spreading ridges. For older times, paleogeographers must rely upon paleomagnetic data referenced to an assumed geocentric, spin-axial dipole magnetic field. There is ample evidence for dominance of this axial dipole field configuration for most of the past 2 Gy (Evans (2006) and references therein). While many authors have used the unfiltered global paleomagnetic database to estimate the maximum permissible contribution of non-dipole terms in the geomagnetic spherical harmonic expansion (e.g., Evans, 1976; Kent and Smethurst, 1998), the likelihood that continents are not distributed uniformly on the globe over time (e.g., Evans, 2005) introduces a ready alternative explanation for the database-wide trends.

Mesozoic–Cenozoic paleogeographic reconstructions usually rely on the collection of a time series of well-dated paleomagnetic poles (called apparent polar wander paths, or APWPs) from distinct continental blocks. When combined with other geological or paleontological constraints, it is possible to match and rotate similarly shaped portions of those paths into overlapping alignment (Irving, 1956; Runcorn, 1956), thereby providing, to first order, the absolute paleolatitude and relative paleolongitude for constituent plate-tectonic blocks of ancient supercontinents such as Pangea. For times prior to the oldest marine magnetic lineations, matching exceptionally quick APWP segments which might correspond to rapid, sustained TPW provides an alternative paleomagnetic method for constraining paleolongitude, relative to the arbitrary meridian of a presumed-equatorial TPW axis (Kirschvink *et al.* (1997) and see subsequent sections).

As discussed subsequently, accumulating evidence suggests that Neoproterozoic and Early Paleozoic time experienced much larger and more rapid TPW episodes than apparent during the Mesozoic and Cenozoic Eras, suggesting fundamental (and intellectually exciting) temporal changes in basic geophysical parameters that control Earth's moment of inertia tensor.

Following theoretical work on 'polar wandering' in the late nineteenth century, Wegener (1929) (English translation by Biram (1966; pp. 158–163)) recognized that continents might appear to drift not only at the behest of spatially varying internal forces, but also by steady or punctuated whole-scale shifting of the solid-Earth reference frame with respect to the ecliptic plane (i.e., the 'celestial' or 'rotational' reference frame):

> ... the geological driving force acts as before and shifts the principal axis of inertia by the amount x in the same direction, and the process repeats itself indefinitely. Instead of a single displacement by the amount x, we now have a *progressive* displacement, whose rate is set by the size of the initial displacement x on the one hand, and by the viscosity of the earth on the other; it does not come to rest until the geological driving force has lost its effect. For example, if this geological cause arose from the addition of a mass m somewhere in the middle latitudes, the axial shift can only cease when this mass increment has reached the equator... p. 158 (italics Wegener's)

Since Earth's geomagnetic field derives directly from its spin influence on convection cells in its liquid outer core, which are sustained by growth of the solid inner core and by plate-tectonics-driven secular mantle cooling (Nimmo, 2002; Stevenson, 1983), TPW causes the Earth's mantle and crust to slip on the solid/liquid interface at core–mantle boundary, while Earth's magnetic field most likely remains geocentric and average spin-axial.

Consequently, TPW was recognized as a possibly confounding signal by early paleomagnetists (Irving, 1957; Runcorn, 1955; Runcorn, 1956), although ultimately TPW was assumed to be negligible relative to rates of plate motion (Irving (1957), DuBois (1957); and most comprehensively Besse and Courtillot (2002)). Short intervals of non-negligible TPW have been hypothesized for various intervals of the Phanerozoic and are permitted by the sometimes-coarse resolution of the global paleomagnetic database (Besse and Courtillot (2002, 2003); and see

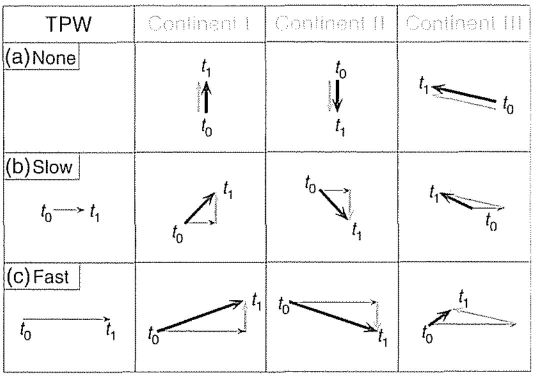

Figure 1 Cartoon showing contribution of TPW to APWP. For zero (a), slow (b), or fast (c) TPW over time increment t_0–t_1 (thin black vectors in top, middle, and bottom rows, respectively), plate-tectonic motion (light gray vectors) may dominate – or be obscured within – the net APW signal. The fidelity by which APW represents plate motion will depend not only on the relative rates of TPW and plate motion, but also on the relative directions in an assumed independent (e.g., geomagnetic) reference frame. Observed coherence of APW between continents with dissimilar plate motion vectors divulges an increased TPW rate. Reprinted from figure 2 in Evans DAD (2003) True polar wander and supercontinents. *Tectonophysics* 362(1–4): 303–320, with permission from Elsevier.

subsequent sections). Irving (1988, 2005) further recounts the historical adoption of paleomagnetism to test hypotheses of continental drift.

In the wake of modern hypotheses suggesting that ancient TPW rates may sometimes match or exceed long-term plate velocities (see subsequent sections), Evans (2003) enunciated the combinatorial possibilities by which TPW may either enhance or mask the plate-tectonic component of APW (**Figure 1**). Most powerfully, TPW must be recognized in the paleomagnetic record as an APW component common to all plates in the celestial or geomagnetic reference frames. Plate-tectonic motion is expected to vary considerably, and even possibly sum to zero (no net rotation) (Gordon, 1987; Jurdy and Van der Voo, 1974, 1975). Lack of kinematic information from ancient areas of oceanic lithosphere that have been lost via subduction precludes rigorous estimation of this no-net-rotation reference frame and thus hinders ancient TPW estimates using that method.

5.14.2.2 'Type 0' TPW: Mass Redistribution at Clock to Millenial Timescales, of Inconsistent Sense

Although not the principal subject of this review, measurable amounts of small-magnitude TPW have been observed to follow major earthquakes that redistribute surficial mass nearly instantaneously (e.g., Soldati *et al.*, 2001). The conservation of momentum response of this variety of TPW is often associated with (and more popularly reported as) changes in the length of day, although specific mass redistributions may change Earth's spin rate though not move its inertial axes. On a neotectonic timescale, earthquake-induced TPW may have no net effect on APW, since fault orientation is controlled by subplate scale stress regimes, which vary globally (although the long-term effect of earthquake-induced TPW might also be nonzero; see, e.g., Spada (1997)).

Very short timescale TPW is also driven by momentum transfer within and between the circulating ocean and atmosphere systems and Earth's solid surface (e.g., Celaya *et al.*, 1999; Fujita *et al.*, 2002; Seitz and Schmidt, 2005). Such varieties of subannual, itinerant TPW are superimposed upon the larger-magnitude annual and Chandler wobbles (e.g., Stacey, 1992), 12 and *c.* 14 month decametric oscillations of ω (e.g., data of the United States Naval Observatory, International Earth Rotation and Reference Systems Service).

On a somewhat longer timescale, glacial ice loading and postglacial isostatic rebound produces lithospheric mass redistribution that drives TPW at the same rate (centimeters per year) as continental plate motions (Mitrovica *et al.*, 2001a, 2001b, 2005; Nakada, 2002; Nakiboglu and Lambeck, 1980; Sabadini and Peltier, 1981; Sabadini, 2002; Sabadini *et al.*, 2002; Vermeersen and Sabadini, 1999). However, the ~10 ky timescale for dampening of isostatic dynamics, and the cyclic nature of Quaternary ice sheets, probably also relegates this TPW to insignificance when examining APW paths over million-year timescales.

Following Evans (2003) and elaborated subsequently, we term all TPW of fleeting duration relative to plate-tectonic timescales or hydrostatic geoid relaxation as 'type 0'. For more detailed treatment of the considerable literature examining type 0 TPW, we point the reader to Spada *et al.* (2006).

5.14.2.3 Type I TPW: Slow/Prolonged TPW

For TPW at timescales and magnitudes relevant to plate tectonics, the effects of surficial and internal mass parcels which dominate changes to Earth's net moment of inertia tensor will vary in part with the square of radial distance. Other contributing factors to the relative effects of such anomalies are somewhat more complicated.

For instance, Hager *et al.* (1985) note that while Earth's nonhydrostatic geoid is dominated by the signature of subducting slabs residing in the upper mantle, the residual geoid (nonhydrostatic geoid minus the modeled contribution of those slabs) correlates with presumed lower-mantle thermal anomalies. Positive dynamic topography at viscosity discontinuities (principally the core–mantle boundary, the crust–mantle boundary, and possibly the 660 km discontinuity) could balance lower-mantle density deficiencies such as rising plumes, while negative dynamic topography at the same discontinuities could counteract upper-mantle density excesses due to slabs (Hager *et al.*, 1985).

A buoyant, upper-mantle plume head illustrates the nontrivial compensatory effects of a density anomaly interacting with surrounding mantle of variable viscosity and structure, in different radial positions. While in the lower mantle, this plume head might have created sufficient positive dynamic topography at the core–mantle boundary and 660 km discontinuity to counteract the negative effect of its inherent density deficiency. When rising through the upper mantle, which is ~10–30 times less viscous than the lower mantle, however, immediate dynamic topographic effects should be diminished. In that case, the density deficiency of the rising mantle plume, plus its greater radial distance, should effectuate a decrease in Earth's inertial moment along the radial axis of plume ascent, whereas only ~10 My earlier, the same mantle plume could have produced a positive inertial anomaly along the same axis.

Moreover, entrainment of surrounding material at the front of and beside moving mantle density anomalies may also either exaggerate or mitigate the effects of those parcels (e.g., Sleep, 1988; Zhong and Hager, 2003), depending on anomaly speed and surrounding mantle viscosity, as well as radial position.

Finally, Earth's inertial tensor is also sensitive to the volumes of density anomalies. Considering both size and location of moving mass components, we might expect mantle superswells to exhibit great, consistently positive effects on Earth's net inertial tensor, whereas lesser and variable magnitude effects could be produced by individual mantle plumes or subducting slabs (**Figure 2**).

Evans (2003) relates these putative geodynamic drivers to a TPW-supercontinent cycle. In the first stage of the cycle, individual cratonic components of a future supercontinent amalgamate at any particular latitude on Earth. During amalgamation, plate-tectonic velocities of already assembled fragments will tend to slow. Consequently, mantle beneath the centroid of a supercontinent will tend to become buoyant, as a result of thermal insulation by the supercontinent and its circumferential, subducting slabs, as well as of upward return flow induced by those sinking slabs (this argument adapts Anderson (1982).

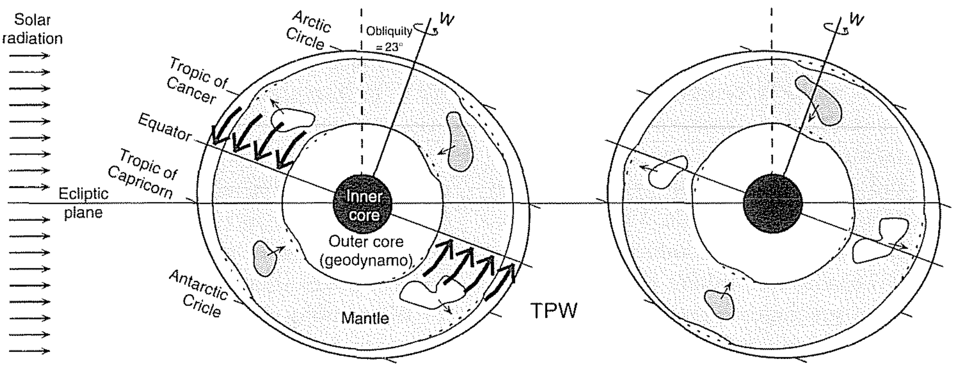

Figure 2 Cartoon of possible mantle phenomena driving TPW. In addition to surface loading, mass redistribution in the mantle also drives changes in Earth's moment of inertia. Entrainment of flowing material along the edges of rising (light) and sinking (dark) mass anomalies will modify their effective contributions. Dynamic topography at viscosity discontinuities leading and trailing the moving anomalies would similarly affect the net inertial change. A dynamic planet (equatorial bulge exaggerated) spins stably and conserves momentum by shifting positive inertial anomalies toward the equator and negative inertial anomalies toward the poles via TPW. Because TPW affects only the solid Earth, whereas Earth's geomagnetic field arises from the vorticity of convection in its liquid outer core, continents will rotate through the geomagnetic and celestial reference frames; while those reference frames remain, on average, fixed with respect to each other. Adapted from figure 1 in Evans DAD (2003) True polar wander and supercontinents. *Tectonophysics* 362(1–4): 303–320.

Elevated dynamic topography from the resulting superswell and the overlying supercontinent that created it will alter Earth's inertial tensor so that slow, continuous TPW places the supercontinent and superswell on Earth's equator (Anderson, 1994; Richards and Engebretson, 1992). Evans (2003) termed this stage of the hypothesized TPW-supercontinent cycle 'type I' TPW.

The Tharsis volcanic region on Mars is plausibly an example of a type I TPW-shifted surface mass (Phillips *et al.*, 2001). In contrast, the south polar water geyser on Saturn's moon Enceladus is an apparent example of the eruption of a hot, buoyant plume associated with migration from mid-latitudes toward a spin-axis (Nimmo and Pappalardo, 2006). Enceladus' mantle is presumably water ice while its core is (mostly nonmolten) silicate and/or iron (Porco *et al.*, 2006). We therefore suggest that the afore-summarized logic of Hager *et al.* (1985) restricts partial silicate melting to Enceladus' uppermost core; or else core diapirism would surely have overwhelmed inertial effects of mantle (ice) upwelling, forcing equator-ward rather than poleward TPW.

5.14.2.4 Type II TPW: Fast/Multiple/Oscillatory TPW: A Distinct Flavor of Inertial Interchange

Once an equatorial-migrated supercontinent begins to fragment, its superswell might remain essentially fixed in an equator-centered position in the angular momentum reference frame (disregarding orbital oscillations), while the constituent continental fragments disperse away from the superswell.

The centroid of that relict superswell would likely define Earth's minimum moment of inertia axis. If Earth's maximum and intermediate inertial axes were of nearly equal moment – dominated by the first harmonic geoid minimum to the superswell and by the uniformly dispersing fragment plates – then incremental changes in one or the other of those approximately equivalent moments might reverse their relative magnitudes, producing an 'intertial interchange' event (Evans *et al.*, 1998; Evans, 2003; Kirschvink *et al.*, 1997; see also Matsuyama *et al.*, 2006).

For instance, individual mantle plume ascents and/or eruptions, orogenic root delaminations, initiation of new subduction on the trailing edge of one dispersing supercontinent fragment but not another, or even changes in the relative sizes and speeds of those fragments might enhance the intermediate inertial moment and cause it to transiently equal or slightly exceed that of Earth's previously maximum (average daily spin) axis.

In such a case, Earth's new, equatorial maximum moment of inertia axis would experience poleward drift in the celestial reference frame, until Earth's inertia tensor satisfied simple spin mechanics once more.

If the mass anomaly of the supercontinental superswell were large enough to pin $\mathbf{I}_{\min}$ stably on the equator, 'normal' plate-tectonic and mantle-dynamic events would continue to enhance one of the other two (nonminimum) inertial moments. Repeated, frequent, and sudden switches of the maximum and intermediate inertial moments could produce multiple episodes of TPW adjustment. Thus aforementioned 'type I' TPW might prepare the planet for multiple 'type II' events that could occur much more frequently than would be predicted by considering only randomly moving internal masses (Anderson (1990, p. 252); Fisher (1974)).

In summary, 'type II' TPW might produce back-and-forth rotation or repeated, same-sense tumbling about an equatorial ($\mathbf{I}_{\min}$) axis over an interval while $\mathbf{I}_{\max} \approx \mathbf{I}_{\text{int}}$. The magnitude of any single event is unpredictable, as it would depend upon the magnitude and duration of the transient changes in the moment of inertia tensor, which in turn are a function of the speed and strength at which the driving anomalies are imposed and compensated.

5.14.2.5 Hypothesized Rapid or Prolonged TPW: Late Paleozoic–Mesozoic

Marcano *et al.* (1999) note that the Pangean APW path tracks ~35° of equator-ward arc from ~295 to ~205 Ma, indicating a corresponding poleward shift of the lithosphere via plate tectonics and/or TPW. We note that ~25° of arc occurs during the latter half of this interval, at an inferred rate of ~0.45° My^{-1}. Because the leading edge of Pangea in such a plate kinematic reconstruction should have overrun a considerable sector of Panthalassan Ocean lithosphere, those authors suggest the subduction-depauperate geologic record of Pangea's Cordilleran–Arctic Margin favors interpretation of the long APW track as relatively fast, sustained TPW. Irving and Irving (1982) made a similar suggestion of anomalous TPW near the Permian–Triassic boundary interval.

We suggest that the apparently poleward motion of Pangea over this interval might be due to TPW motion caused by upper-mantle ascent of the Siberian Traps plume. For a plume-consistent model incorporating marine accommodation of much early Siberian Trap stratigraphy, see Elkins-Tanton and Hager (2005). Such a plume might have originated in the lower mantle yet avoided triggering equator-ward TPW as discussed previously if I_{max} had significantly exceeded I_{int} during lower-mantle plume ascent, though the two inertial moments converged prior to ~251 Ma.

Perhaps the span of this hypothesized Permian–Triassic Pangea-poleward TPW (≥55 My) corresponds to the minimum timescale for buildup of thermal insulation, reflected by later equator-ward APW of the North American Jurassic APW cusps (Beck and Housen, 2003) and possible correlatives on other, less-constrained continents (Besse and Courtillot, 2002), although see Hynes (1990) and subsequent discussion. It is certainly worth testing this scenario with high-resolution paleomagnetic studies in the Permian/Triassic boundary interval, particularly from sedimentary sections that have preserved stable components of that age (e.g.,Ward *et al.*, 2005).

For the post-200 Ma global paleomagnetic record, in which a fixed hot-spot reference frame may be hypothesized in order to model true plate-tectonic drift with respect to the mesosphere, Besse and Courtillot (2002, 2003) have presented the most recent thoroughly integrated database and discussion (e.g. Andrews *et al.*, 2006; Besse and Courtillot, 1991; Camps *et al.*, 2002; Cottrell and Tarduno, 2000; Dickman, 1979; Gordon *et al.*, 1984; Gordon, 1987, 1995; Harrison and Lindh, 1982; Prevot *et al.*, 2000; Schult and Gordon, 1984; Tarduno and Smirnov, 2001, 2002; Torsvik *et al.*, 2002; Van Fossen and Kent, 1992). Besse and Courtillot (2002) critically discuss hypothesized Cretaceous fast TPW and provide in-depth consideration of tests and caveats that are only summarized here.

In brief, while many authors have noted that hot spots may form a significantly nonuniform reference frame (e.g., recently Cottrell and Tarduno, 2003; Riisager *et al.*, 2003; Tarduno and Gee, 1995; Tarduno and Cottrell, 1997; Tarduno and Smirnov, 2001; Tarduno *et al.*, 2003, Besse and Courtillot (2002) base their synthesis upon Indo-Atlantic hot spots, which appear more fixed to each other than they are to Pacific hot spots (Muller *et al.*, 1993). Some Pacific hot-spot-motion models, (e.g., DiVenere and Kent, 1999; Petronotis and Gordon, 1999) are similar to Besse and Courtillot's (2002) Indo-Atlantic hot-spot APWP, although Van Fossen and Kent (1992) argue for incompatibility of the two oceanic reference frames. Ultimately, whether or not hot-spot motion represents coherent or independent drifting in a 'mantle wind', TPW of the whole solid Earth in the geomagnetic/celestial reference frame should still be resolvable if it is rapid or long-lived, by discerning common APW tracks from all continents.

Hynes (1990) invokes a sort of TPW for Early Jurassic time, *c.* 180–150 Ma, but latter compilations based on better-constrained hot-spot age and position data mark the same period as a standstill (e.g., Besse and Courtillot, 2002). The post-140 Ma interval, which Hynes (1990) marks as a standstill, appears strongest as prolonged, possibly slow TPW in those later models. Since the seafloor hot-spot record before ~150 Ma is poor, and continental hot-spot tracks may be subject to eruptive-tectonic complications, Hynes' (1990) Jurassic-TPW event is of questionable support. Recent studies in lower Jurassic South American strata (Llanos *et al.*, 2006) and Upper Jurassic–Early Cretaceous successions of Adria (Satolli *et al.*, 2007) appear to support possible bursts of fast TPW during this interval.

Both Besse and Courtillot (2002) and Prevot *et al.* (2000), however, mark the Middle Cretaceous as an interval over which TPW appears to have sustained a net faster, coherent component of motion in the geomagnetic (celestial) reference frame (~<0.5° My^{-1}) than during TPW-stillstand intervals before and afterward. In both studies, the authors note that even a global synthetic APWP lacks the time resolution (and for some intervals, global pole coverage and/or paleomagnetic pole precision) necessary to discriminate very short, rapid TPW events from somewhat longer (~5–10 My) events of slower pace. Thus, while Prevot *et al.* (2000) favor a short interval of still-quicker TPW at ~115 Ma, the conceptual introduction of oscillatory, type II TPW, further complicates such recognition.

Besse and Courtillot (2002) favor conservative interpretation of the synthetic global APWP dataset and ascribe part or all of Prevot's ~115 Ma event to a small number of data bracketing the interval, and/or to inaccurate dating of supposedly 118–114 Ma, petrologically dissimilar kimberlites in South Africa.

Petronotis and Gordon (1999) and Sager and Koppers (2000a) hypothesize very fast TPW between 80–70 Ma, and near 84 Ma, respectively, possibly as the middle of an oscillatory, triple event. Cottrell and Tarduno (2000) emphasize those authors' enumeration of potential ambiguities and pitfalls of magnetic anomaly modeling and age dating of seamounts (but see Andrews *et al.* (2006) for a promising new treatment), and suggest that hypothesized Campanian–Maastrichtian TPW events fail a global signal test when compared with magnetostratigraphic data from Italy (e.g., Alvarez *et al.*, 1977; Alvarez and Lowrie, 1978). Sager and Koppers (2000b) question whether that Italian magnetostratigraphic data are of sufficient precision to rule out all possible interpretations of the Pacific seamount dataset, within its own uncertainty.

The apparent dispersion of Pacific paleomagnetic data, hypothetically accounted for by TPW, remains unresolved in still more recent studies (Sager, 2006). The younger (<85 Ma) interval of Cretaceous TPW ought to be readily testable by new magnetostratigraphies from various continents to parallel the classic Italian sections. Detailed magnetostratigraphic analysis of Paleocene–Eocene transitional sections exposed on continents led Moreau *et al.* (2007) to hypothesize small-magnitude, fast, back-and-forth TPW during that time, a possibility which may also be supported by paleomagnetic data from the North Atlantic Igneous Province (Riisager *et al.*, 2002).

5.14.2.6 Hypothesized Rapid or Prolonged TPW: 'Cryogenian'–Ediacaran–Cambrian–Early Paleozoic

Substantial evidence is accumulating that Earth experienced large and rapid bursts of TPW during Neoproterozoic and Early Paleozoic time, of a sort that perhaps has not been experienced since. This 'type II' TPW, invoked as a single event through Early- to Mid-Cambrian time by Kirschvink *et al.* (1997) and debated by Torsvik *et al.* (1998), Evans *et al.* (1998), and Meert (1999), was originally termed inertial interchange true polar wander ('IITPW',). We prefer Evans' (2003) renaming of the process principally because it de-emphasizes the reference frame of the pre-TPW inertial tensor.

Per Kirschvink *et al.* (1997) 'interchange', refers to the beginning of such TPW, when the maximum and intermediate inertial moments of that tensor's reference frame switch identities. One frequent misconception has been that, consequently, the TPW response of the solid Earth must be a before-to-after change of 90°. As noted in, for example, Evans *et al.* (1998) and Matsuyama *et al.* (2006), that change may be any magnitude of rotation at all less than 90°, and continuing until new axes are definable and stable, orthogonal from each other and from the (effectively stationary) equatorial, $\mathbf{I}_{\min}$. The end-member case of a 90° shift would imply that the positive mass anomaly causing the shift was imposed precisely along the spin-axis (as might be the case with an upper-mantle plume head). Off-axis eruption would lead to smaller magnitude events.

We prefer renaming Kirschvink *et al.*'s (1997)'s 'IITPW' as 'type II' TPW also to emphasize its hypothesized proclivity to multiple events and to differentiate it from other patterns, as per Sections 5.14.2.5 and 5.14.2.4.

The hypothesized pan-Cambrian type II TPW event of Kirschvink *et al.* (1997) defines an approximate $\mathbf{I}_{\min}$ axis (the 'TPW axis'). Evans (2003) notes that this TPW axis is essentially identical to both a plausible centroid of the supercontinent of Rodinia, as well as that hypothesized in the reference frame of the largest Early Paleozoic continent, Gondwanaland, by Van der Voo (1994). (Also see Veevers (2004) and later Piper (2006) and **Figure 3** here; and see subsequent sections.)

That coincidence of the Van der Voo (1994) and Kirschvink *et al.* (1997) TPW axes was invoked as an example of the potential long-lived legacy of supercontinental superswell geoid anomalies by Evans (2003), also citing, as a modern analog, Pangea's relict

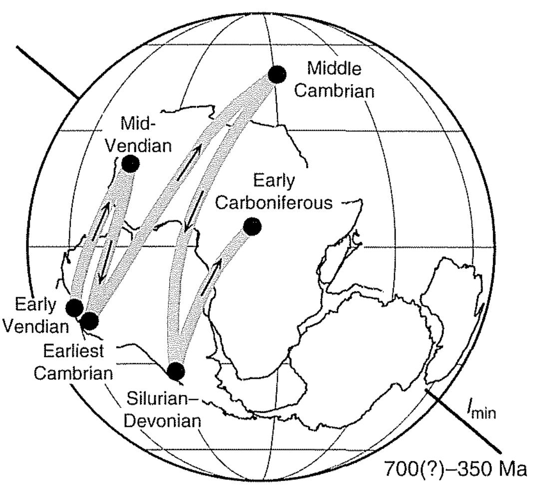

Figure 3 Stability of $\mathbf{I}_{\min}$. Van der Voo (1994) notes that Gondwanaland's Cambrian–Carboniferous APWP includes dramatic excursions; and Kirschvink *et al.* (1997) and Evans (1998, 2003) note that Late Neoproterozoic–Cambrian paleopole dispersion marks swings with approximately the same orientation. Evans (2003) suggests that all those swings might represent type II TPW about a paleo-equatorial minimum moment-of-inertia axis defined by a mantle superswell legacy of the Neoproterozoic supercontinent, Rodinia. From figure 3 in Evans DAD (2003) True polar wander and supercontinents. *Tectonophysics* 362(1–4): 303–320.

geoid persisting to the present (Anderson, 1982; Chase and Sprowl, 1983; Davies, 1984; Richards and Engebretson, 1992). Whether relict from a large Ediacaran–Cambrian continent or from the earlier supercontinent Rodinia, Evans and Kirschvink (1999) and Evans (2003) note that, in fact, at least three distinct TPW pulses (of apparently alternating sense) are implied for both Late Neoproterozoic and Early Paleozoic time.

Oscillatory, rapid TPW about an equatorial axis has also been invoked to explain stratigraphically systematic but $\geq 50°$ dispersed paleomagnetic poles produced from Svalbard's Akademikerbreen succession deposited on Rodinia's margin *c.* 800 Ma (Maloof *et al.*, 2006). With primary remanence established by a positive syn-sedimentary fold test and by apparently correlatable polarity reversals, this result is highly robust. Although the sequence is undated except by stratigraphic and carbon isotopic correlations to two Australian sub-basins, inferred TPW events appear rapid on a sequence-stratigraphic timescale. Using global carbon isotope correlation and thermal subsidence analysis, the TPW event-recurrence timescale is estimated at $<<15$ My.

Li *et al.* (2004) invoke type I TPW to explain dramatic paleomagnetic difference between South China's high paleolatitude, 802 ± 10 Ma Xiaofeng dikes and unconformably overlying, gently tilted, low paleolatitude, 748 ± 12 Ma Liantuo glacial deposits (Evans *et al.*, 2000; Piper and Zhang, 1999); and see subsequent sections. Although the age of Li *et al.*'s (2004) hypothesized TPW is imprecisely constrained, and Maloof *et al.*'s (2006) hypothesized events are not dated directly, the two studies appear to invoke different types of TPW for, essentially, a single phase of a supercontinent cycle at *c.* 800 Ma. Large uncertainties in the absolute ages of the Svalbard succession studied by Maloof *et al.* preclude precise correlations to the South China poles; furthermore, uncertainties in Rodinia paleogeography (e.g., Pisarevsky *et al.*, 2003) leave considerable flexibility for reconstructing South China relative to Laurentia (including Svalbard). Identifying the type (I vs II) of TPW at *c.* 800 Ma, and inferring its dynamic cause, must await better constraints in these two topics.

5.14.2.7 Hypothesized Rapid or Prolonged TPW: Archean to Mesoproterozoic

Evans (2003) suggests that long tracks and loops of Laurentia's Mesoproterozoic APWP might represent oscillatory TPW in the inertial legacy of Earth's Paleoproterozoic supercontinent, Nuna, although global paleomagnetic database synthesis testing of such a hypothesis has yet to be presented robustly.

Considering the oldest volcanic succession with detailed strata-bound paleomagnetic analyses, Strik *et al.* (2003) note that one of several unconformities punctuating the basalt series of Pilbara's late Geon 27 Fortescue Group separates zones of distinct magnetization direction, but with similar petrographic character, marked by a $\sim 27°$ inclination difference across ~ 3 My. These authors enumerate rapid TPW as one possible explanation, although they prefer alternative scenarios.

5.14.3 Geodynamic and Geologic Effects and Inferences

5.14.3.1 Precision of TPW Magnitude and Rate Estimation

The magnitude and rate of type 0 TPW are directly measured or derived quantities. Precision is often limited, in practice, by technical capabilities of geodetic and satellite instruments. In principle it is ultimately limited by uncertainties in fundamental constants like g, and by observational design, which may not readily quantify special relativistic effects. These uncertainties are probably trivial for the purposes of any geologic application of type 0 TPW data.

The magnitude and rate of type I and II TPW are controlled by the same processes, although we expect type I TPW to be slower than type II. This is because the hypothesized forcing (long-wavelength mantle upwelling in context of initial $I_{min} \approx I_{int}$) is more slowly imposed. Both phenomena should be inherently rate limited by the speed at which Earth's viscoelastic daily-rotational bulge can relax through the incrementally shifting solid Earth. Both phenomena should be resolved in magnitude and rate at the lowest limits of paleomagnetic and geochronologic error and uncertainty.

Quantifying the viscoelastic rate control on type I and II TPW is nontrivial. The three controlling variables are probably forcing magnitude of inertial changes, timescale of inertial change, and effective mantle viscosity (Tsai and Stevenson (2007), expanding on Munk and MacDonald (1960)). Most TPW numerical models assume a single viscosity or two-layered viscosity for the solid Earth; at any rate, there is no consensus on the precise viscosity structure of the modern mantle. We argue that these models might equally well be driven by empirical paleomagnetic data as vice versa.

Simplified mantle modeling confirms that lesser effective mantle viscosity permits faster TPW and that more highly structured mantle viscosity enhances sensitivity to a given forcing (because of the dynamic topography and surrounding entrainment effects). The balance between those influences, however, is unclear. Given a mantle viscosity structure (e.g., Mitrovica and Forte, 2004), simple TPW rate limitation calculations (e.g., Spada *et al.*, 2006; Spada and Boschi, 2006; Steinberger and Oconnell, 1997) may be controlled by average mantle viscosity or perhaps maximum viscosity. Obviously, more experimental and theoretical work is needed on this question.

We project the possible shape of a TPW rate-limitation versus controlling viscosity curve onto Mitrovica and Forte (2004) mantle viscosity structure in such a way that suggests, today, full type I (i.e., pole-to-equator) TPW could occur over an order of magnitude different timescales, within the span of possible controlling mantle viscosity (**Figure 4**).

Besse and Courtillot (2002) synthesize the global paleomagnetic record over the past 200 My, and consider the most conservative solid Earth (e.g., Indo-Atlantic hot spot) reference frame in their analysis. TPW appears to be an episodically measurable contributor to APW. Over 'fast' TPW intervals estimated to last ~20–40(?) My, TPW may occur at $<0.5^\circ\ \mathrm{My}^{-1}$. As already discussed, those authors acknowledge that time resolution in the global coverage of the paleomagnetic database limits their analysis to moving 5 or 10 My windows at finest resolution. If faster TPW occurred over a shorter timescale, it would not be readily recognized using a time-averaged approach.

If ancient TPW were estimated – by APWP compilation in older times or by single-location paleomagnetic records of any age – to occur substantially quicker, then it should be possible to use the TPW data to construct inverse models of the controlling mantle viscosity. This approach might allow constraints to be placed on mantle viscosity and related parameters as a function of geological time.

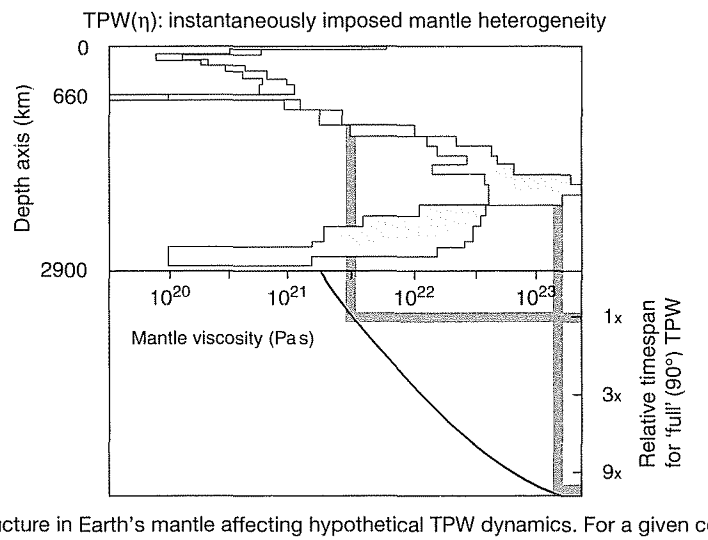

Figure 4 Viscosity structure in Earth's mantle affecting hypothetical TPW dynamics. For a given controlling mantle viscosity, maximum TPW rate may be modeled (red curve). In the cartoon representation shown here, present-day TPW controlled by mantle viscosity of $\sim10^{23}$ Pa s would span a given arc of rotation ~10 times slower than TPW controlled by mantle viscosity of $\sim2 \times 10^{21}$ Pa s. The viscosity structure of Earth's modern mantle is uncertain in sense and magnitude at many levels, particularly in the deep mantle. Mitrovica and Forte (2004), however, suggest a dual inverse-modeled mantle viscosity structure as depicted in yellow (with viscosity uncertainties occupying horizontal space and mantle position and thickness varying vertically). It is not clear to us whether a highly structured mantle, such as is inferred for modern Earth, would be effectively 'controlled' by its maximum-viscosity shell, or whether it will be controlled by some integrated average viscosity, permitting faster net TPW. Projection of ever-more refined TPW rate-response calculations and ever-more sophisticated viscosity structure models is critical to understanding the putative TPW rate limitation on modern Earth. If ancient TPW is demonstrated to occur at significantly faster rates, secular evolution of controlling mantle viscosity (or development of viscosity structure) could be inferred and inversely modeled. Adapted from figure 4(b) in Mitrovica JX and Forte AM (2004) A new inference of mantle viscosity based upon joint inversion of convection and glacial isostatic adjustment data. *Earth and Planetary Science Letters* 225(1–2): 177–189.

5.14.3.2 Physical Oceanographic Effects: Sea Level and Circulation

George Darwin (1877) was the first to note that changes in Earth's rotation would induce fluctuations in local sea level. In reviewing these early studies that specifically contrasted the delayed response of the solid Earth's viscoelastic bulge compared with the immediate response of the ocean's bulge to changes in the spin vector, we again return to the prophetic words of Alfred Wegener (Biram, 1966; translated from Wegener (1929)):

> ... Since the ocean follows immediately any re-orientation of the equatorial bulge, but the earth does not, then in the quadrant in front of the wandering pole increasing regression or formation of dry land prevails; in the quadrant behind, increasing transgression or inundation. (p. 159)

The physics of this effect have been subsequently modeled with increasing sophistication (Gold, 1955; Mound and Mitrovica, 1998; Mound *et al.*, 1999, 2001, 2003; Sabadini *et al.*, 1990).

Consider only the magnitude of the spin vector, ω. A simple decrease in magnitude of ω (which is an increase in the length of day without any associated TPW) will reduce the size of Earth's equatorial bulge. However, because the solid Earth is viscoeleastic, it requires $\sim 10^4$ to 10^5 years to fully relax, whereas Earth's ocean surface responds instantaneously. Hence, in equatorial regions, mean sea level will experience a transient relative fall with respect to the land surface, with a compensating rise at higher latitudes. Similarly, simply increasing ω (shortening the day) will produce the opposite effect of equatorial transgressions and high-latitude regressions (Peltier, 1998).

In contrast, altering the orientation of the spin vector relative to the equatorial bulge yields a quadrature pattern in relative sea level. As the ω vector remains constant, dimensions of the overall bulge also remain the same. A point moving toward the equator, for example, will impinge onto the equatorial bulge, and hence tend to increase its distance from the spin-axis.

The solid Earth beneath this point, however, responds with the aforementioned viscoelastic time constant and will lag the ocean's instantaneous shift to the new, itinerant equilibrium shape. That response difference generates a marine transgression. Similarly, points on Earth's surface that move away from the equator during TPW vacate the spin bulge and will relax at the solid Earth's timescale while the adjacent ocean surface 'falls' faster, effecting a regression.

The maximum relative sea-level effect for an instantaneous (and impossible!) shift of exactly 90° would simply be the size of Earth's equatorial bulge, or $\sim$10 km. In reality, sea-level excursions are constrained by the effective elastic lithosphere thickness and viscosity structure of the mantle. Mound *et al.* (1999) estimate that, for reasonable estimates of present viscosity structure, a 90° TPW event acting over 10 and 30 My will generate >200 to $\sim$50 m excursions, respectively (**Figure 5**). TPW sea-level effects

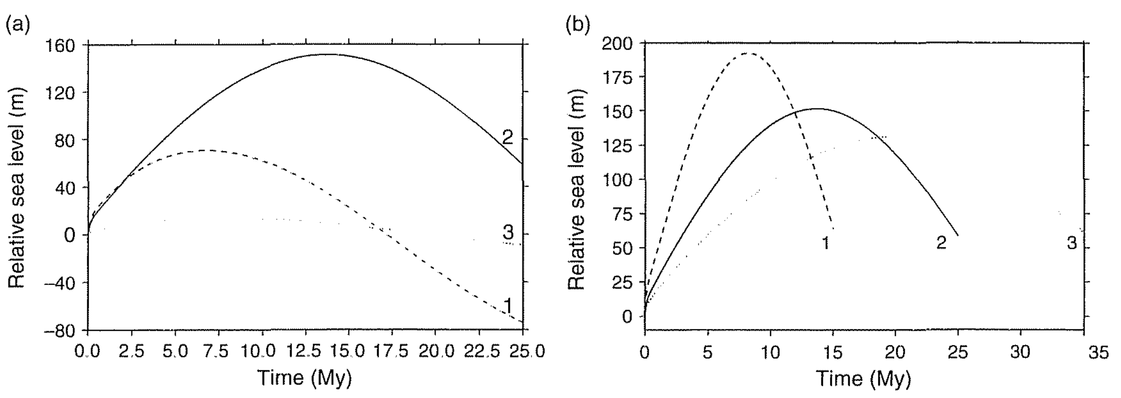

Figure 5 Sea-level fluctuations as a function of TPW rate. (a) Modeled sea-level fluctuations over 25 My of TPW for three locations on the globe: (1), a continent initially at mid-latitude moving through the equatorial bulge to mid-latitudes in the opposite hemisphere, experiences moderate transgression followed by significant regression; (2), an initially polar continent moving toward the equator experiences significant transgression followed by moderate regression; and (3), a continent near the TPW axis experiences little sea-level fluctuation. The period and amplitude of each anomaly in this model are most sensitive to input parameters of lithospheric thickness, upper-mantle viscosity, and TPW rate. (b) The amplitude of any one continent's sea-level anomaly increases nonlinearly with TPW rate, other variables held constant. From figure 2 in Mound JE, *et al.* (1999) A sea-level test for inertial interchange true polar wander events. *Geophysical Journal International* 136(3): F5–F10.

are certainly of equivalent magnitude, and perhaps larger, than those of standard glacioeustasy and should exert first-order control of global sequence stratigraphy during intervals of time for which TPW was significant, quick, and/or frequent.

Estimates of the sea-level effects of the fastest possible TPW motions tend to flounder on the uncertainties of detailed mantle-viscosity structure, but excursions of approximately several kilometers in scale might be feasible for TPW events on the 1–3 My timescale (Kirschvink *et al.*, 2005; Mound *et al.*, 1999). Of course, sea level will relax to roughly its initial state when a TPW event ends.

Physical oceanography should also show second-order responses to TPW. Earth's spin vector modulates a variety of oceanographic parameters, including temperature, the pole-to-equator atmospheric energy gradient, and the chemical dynamics of the world ocean (e.g., mean and local salinity). It also has a large influence on the tides, which depend on the orientation and character of seafloor topography and continental geography. The well-known poleward boundary currents on east-facing continental margins and deepwater upwellings on west-facing margins are fundamental outcomes of Earth's sense of spin. Large TPW events will force changes in many of these parameters that could leave fingerprints in the geological record (**Figure 6**).

During TPW events, we expect thermohaline circulation in the ocean to reorganize – possibly several times – at considerably shorter timescales than the TPW events and possibly at shorter timescales than the resulting sea-level fluctuations. As originally west-facing margins near the equator rotate clockwise, upwelling will cease on those margins and may begin anew on the west-rotating, originally southern margins of the continent in consideration. Boundary currents driving basinal sediment advection may reorganize, foundering or winnowing sand drifts, as low-latitude east-facing continental margins migrate

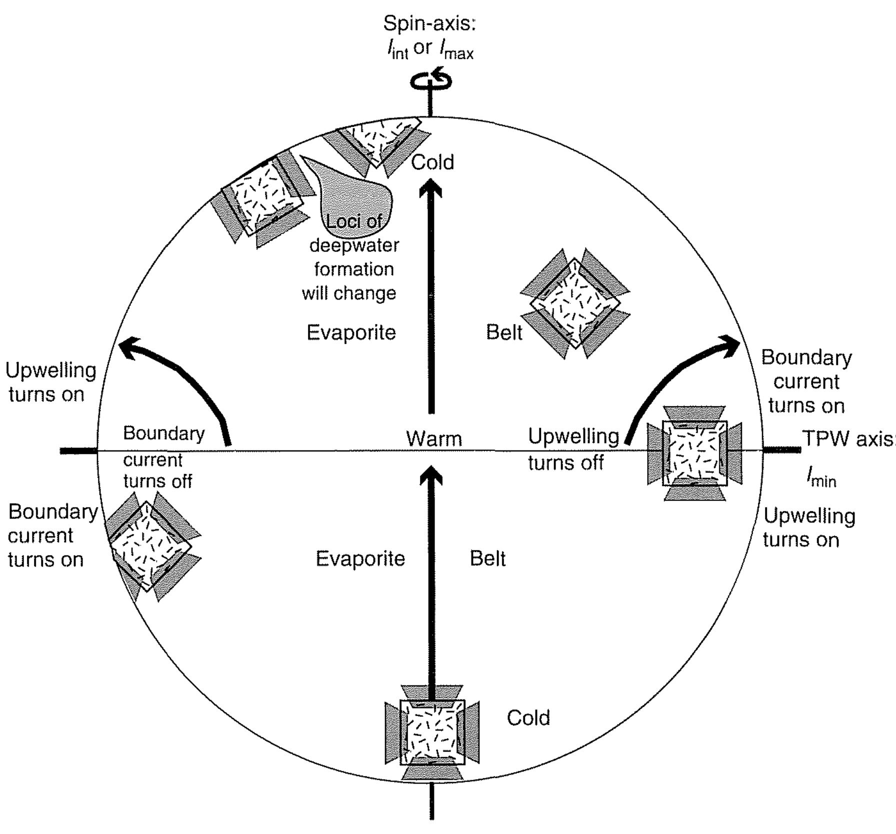

Figure 6 A wide range of first-order physical and chemical oceanographic changes may accompany sea-level fluctuations during TPW, depending on the initial location of a continental margin with respect to the TPW spin-axis. Sediment supply to margins initially girdled by eastern boundary currents may founder; nutrient-rich upwellings on initially west-facing margins may cease and begin anew on initially zonal, later west-facing margins. In general, TPW is expected to leave a legacy of eddy instability and thermohaline reorganization which proceeds episodically during and possibly after an inertial shift.

to polar regions, cross the equator, or rotate into zonality. **Figure 6** illustrates some of the wide range of effects conceivable during a TPW event for distinct continents occupying various original geographic locations. Certainly, hypothesized ancient TPW ought to leave dramatic sedimentological and geochemical signatures in the eu- and miogeoclinal records of most then-extant passive margins (see also Section 5.14.3.3).

At a dramatic extreme, Li *et al.* (2004) follow Schrag *et al.*'s (2002) geochemical modeling and suggest that *c.* 800–750 Ma TPW may have initiated the 'Snowball Earth' glaciations of the Cryogenian Period. Kirschvink and Raub (2003) invoke changes in eddy circulation and lateral sediment advection, as well as permafrost transgression during multiple Ediacaran–Cambrian TPW to destabilize methane clathrates, increase organic carbon remineralizatoin, and effect 'planetary thermal cycling' on the biosphere. In turn, this stimulated the Cambrian Explosion by alternately stressing species and forcing them to reduce generation time, accumulating genetic mutations which would promote morphological disparity and speciation.

5.14.3.3 Chemical Oceanographic Effects: Carbon Oxidation and Burial

As noted in Section 5.14.3.2, TPW is capable of producing a variety of effects on global sea level, ranging from small, meter-scale regional fluctuations associated with isostatic effects from glacial loading and unloading, to possibly larger, even kilometer-scale effects from rapid and 'ultra'-rapid TPW. In turn, sea-level fluctuations can force shoreline migration, alter drainage patterns, and cause geological organic carbon to be remineralized. Potentially, this remineralized carbon could come from bitumens, kerogen, or pressure-destabilized methane clathrates.

As discussed previously, Maloof *et al.* (2006) provide a compelling case for a pair of rapid TPW events in Middle Neoproterozoic platform carbonates of East Svalbard, Norway. Several profiles through the ~650 m thick section record a clear step-function offset in the $\delta^{13}C$ signature of approximately −5‰ identified as the ~800 Ma Bitter Springs Event (Halverson *et al.*, 2005), which lasted ~10 My based on thermal subsidence modeling and younger chronostratigraphic correlations (**Figure 7**).

In Svalbard this isotope shift is bracketed by two sequence boundaries (sea-level erosional horizons). Although magnetization directions before and after the Bitter Springs Event in the Akademikerbreen Group are similar to each other, precisely at these sequence boundaries the mean magnetic declination rotates >50°. Maloof *et al.* (2006) note that this rotation is present in three separate stratigraphic sections separated by >100 km on a single craton, with congruent carbon isotope signals. A pair of rapid TPW events separated by ~10 My provide a single, unified explanation for two important observations.

First, TPW can account for the Bitter Springs isotope anomaly by producing a sudden shift in the fraction of global carbon burial expressed as organic carbon deposition (f_{org}), plausibly by changing the proportion of riverine sediment (and nutrients) deposited at low-latitude versus at mid-latitudes. Per gram of sediment, low-latitude rivers are more effective at organic carbon burial than those at mid- or high-latitudes (Halverson *et al.*, 2002; Maloof *et al.*, 2006). Although paleomagnetic data argue Svalbard was close to the $\mathbf{I}_{\mathbf{min}}$ inertial axis, a 50° type II TPW event could swing pan-hemispheric Rodinia, shifting orographic precipitation loci, drainage patterns, and continental sediment delta locations, varying f_{org}.

Second, this pair of type II TPW events would produce transient sea-level variations. Only two sequence boundaries exist in this interval in Svalbard, and they bracket the isotope anomaly. As discussed previously, Li *et al.* (2004) have also argued for rapid TPW in this general interval of time.

On a more speculative note, Kirschvink and Raub (2003) suggested that a hypothesized interval of multiple, type II TPW may have been in part responsible for the production of large and episodic oscillations in inorganic $\delta^{13}C$ during Early Cambrian time, the so-called Cambrian Carbon Cycles (Brasier *et al.*, 1994; Kirschvink *et al.*, 1991; Magaritz *et al.*, 1986, 1991; Maloof *et al.*, 2005). The principal mechanism suggested – remineralization of organic carbon from exposed sediments and/or destabilization of methane clathrate reservoirs along continental margins and in permafrost – was patterned after similar suggestions for methane release associated with a marked inorganic carbon anomaly at the initial Eocene thermal maximum (IETM, formerly called the Paleocene–Eocene thermal maximum, PETM) event (Dickens *et al.*, 1995, 1997).

Subsequent analyses have questioned this interpretation for the IETM event, based on revised estimates of the available methane reservoir stored in Late Mesozoic and Early Tertiary continental shelf and upper-slope sediments, methane clathrate residence times, and the short (decadal) residence time of methane in Earth's present atmosphere

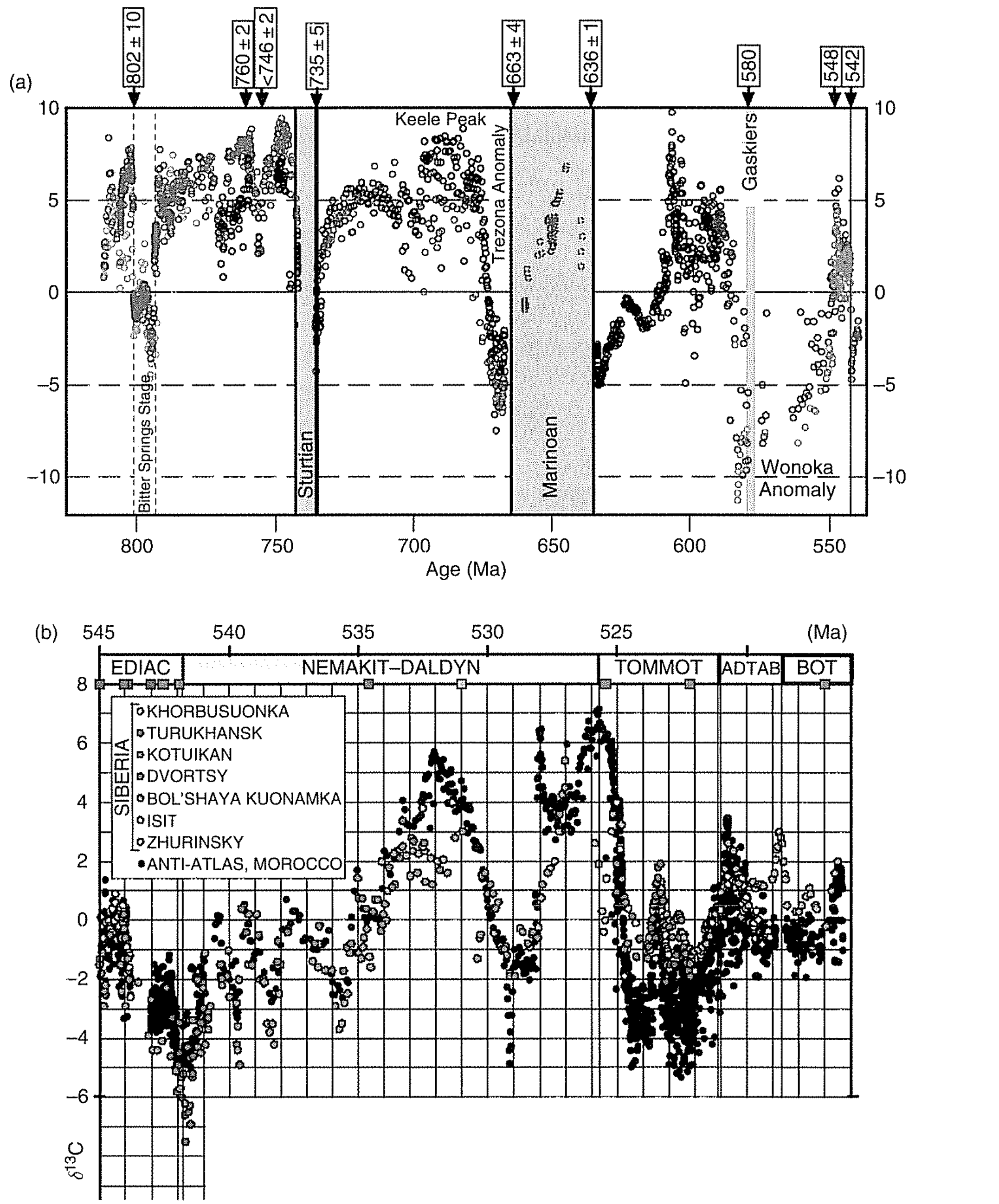

Figure 7 TPW effects on the geological carbon cycle. (a) One possible global inorganic carbon isotopic evolution time series through Mid- and Late-Neoproterozoic time. At least three distinct glacial events punctuate this interval. While successions around the world are ever-better dated by high-precision U–Pb ages on magmatic zircons in interbedded ashes and volcanic flows, ambiguities still exist in sequence-stratigraphic and lithostratigraphic correlations between continents. (As discussed in the text and in captions to **Figures 6** and **7**, global sequence stratigraphic correlations may be severely complicated by TPW.) Maloof *et al.* (2006) consider the long-lived negative carbon isotopic excursion dubbed 'Bitter Springs Stage' a consequence of type II TPW, see text. (b) Cambrian inorganic carbon isotopic evolution time series from well-dated successions in Morocco and undated successions in Siberia. Kirschvink and Raub (2003) note that organic carbon-based isotope curves over parts of the same time interval from Western United States and other areas share many similarly shaped and positioned excursions. Those authors hypothesize that some or all of the negative carbon isotopic excursions in Cambrian time were partly driven by destabilization of seafloor and permafrost methane clathrates during a legacy of eddy instability and thermohaline reorganization associated with Ediacaran–Cambrian type II TPW. Adapted from figure 15(b) in Halverson *et al.* (2005); and part of figure 8 in Maloof AC, *et al.* (2005).

relative to the apparent ~100 000 + interval of initial Eocene carbon isotopic excursion (Buffett and Archer, 2004; Farley and Eltgroth, 2003). In reviewing the controversy, Higgins and Schrag (2006) argue for the sudden close-off of an epicontinental seaway through tectonic action to provide ~5000 Gt of organic carbon needed to produce the effect.

We note here that Kirschvink and Raub's (2003) TPW-based 'methane fuse hypothesis' for the Cambrian anticipated many of the arguments against methane summarized by Higgins and Schrag (2005). Several factors argue that the geological context of the multiple Cambrian carbon cycles are markedly different than the singular end-Paleocene event, in our view making at least the partial involvement of a methane-derived light isotopic reservoir more plausible.

First, Neoproterozoic time (including the Ediacaran Period) is characterized by extended intervals during which the inorganic $\delta^{13}C$ remained markedly positive (+2– +5‰), most likely implying relatively high organic carbon burial fractions, plausibly leading to order-of-magnitude larger methane reservoirs than extant. The long-term average inorganic carbon isotopic value for most of the Phanerozoic Eon is 0‰.

Second, Cambrian cycles are individually no longer, though collectively more prolonged, than Phanerozoic negative carbon isotopic excursions, with at least 12 named cycles up to Middle Cambrian time (Brasier *et al.*, 1994; Montanez *et al.*, 2000) spanning an interval of ~15–20 Ma. When viewed at exceptionally high resolution (e.g., Maloof *et al.*, 2005), many individual Cambrian carbon cycles likely have duration 100 ky–1 My, but with occasional sharp excursions superimposed, reminiscent of the Early Eocene event superimposed on its still-longer Early Eocene climate optimum oscillation. We suspect that the carbon isotopic oscillations discovered recently in the Early Triassic (Payne *et al.*, 2004) are individually of longer average duration, but occur over a shorter overall chronologic interval, than those of the Early Cambrian. The reservoir arguments against methane contributing to the initial Eocene carbon excursion, then, do not apply equally well when applied to Ediacaran–Cambrian time; the geological and physiographic conditions are distinctly different.

TPW-induced changes to the geological carbon cycle are likely to be myriad, with potential positive feedbacks. **Figure 8** elaborates the pervasive, systematic perturbations to the geological carbon cycle expected during TPW-driven sea-level fluctuations

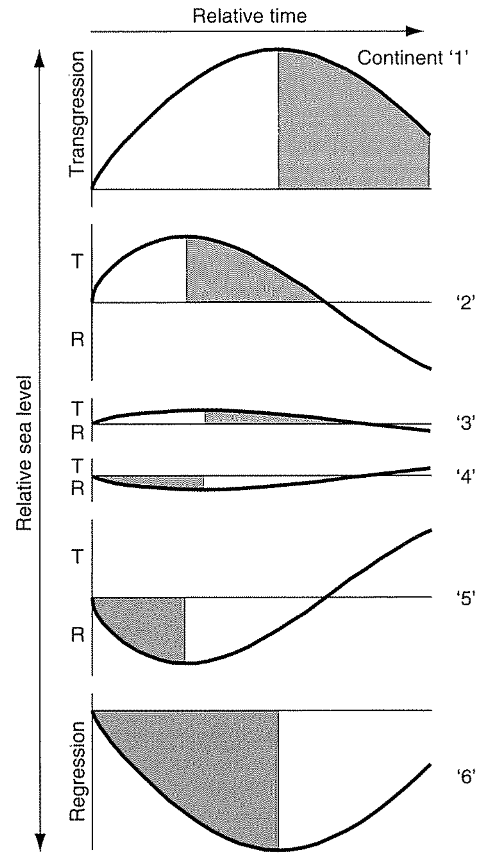

Figure 8 Cartoon elaboration on systematic perturbations to the geological carbon cycle caused by TPW-driven sea-level fluctuations. For schematic sea-level anomalies experienced by continents in six different locations relative to a TPW axis, a different interval of each anomaly will be most susceptible to regression-induced methane clathrate destabilization and oxidation of long-buried organic matter (green); to new burial of organic carbon on TPW-transgressed shelves (white); and subsequent oxidation of part of the same organic-carbon pool during later emergence (blue); and to renewed oxidation of ancient organic matter (yellow). Destabilization of methane clathrate in permafrost, not explicated in this figure, is probably preferred at the very beginning of such a cycle for appropriate continents. Depending on the initial sizes and mean isotopic values of each reservoir, the rate and duration of TPW, and specific parameters including paleogeography and thermohaline circulation, it is possible to imagine (or quantitatively model) a wide range of global inorganic-carbon reservoir isotopic responses. Continent #1 moves from either of Earth's poles to its equator. Continent #2 swings from mid-latitudes on one side of the equator to mid-latitudes in the opposite hemisphere. Continent #3, located near the TPW axis, rotates slightly further away from the equator. Continent #4, located near the TPW axis, rotates slightly closer toward the equator. Continent #5 swings from mid-latitudes across the pole to mid-latitudes in the same hemisphere, but on the opposite side of the globe. Continent #6 moves from near Earth's equator to one of its poles.

for continents in six distinct locations relative to a TPW axis. Some continents will be especially prone to regression-induced methane clathrate destabilization and oxidation of long-buried organic matter; while others will dominantly accommodate new burial of organic carbon on newly TPW-transgressed shelves. If the continental location is appropriate and TPW sufficiently rapid, then TPW transgression may flood continental highlands of exceptionally large area. That same organic carbon pool may oxidize during later emergence related to sea-level reequilibration; other continents may only remineralize ancient organic matter for the first time in the TPW event near its end.

Depending on the initial sizes and mean isotopic values of each reservoir, the rate and duration of TPW, and specific parameters including paleogeography and thermohaline circulation, it is possible to imagine (or quantitatively model) a wide range of global inorganic-carbon reservoir isotopic responses. If a global Ediacaran–Cambrian paleogeography were confidently reconstructed, box modeling of reservoirs over relative timescales as indicated in **Figure 8** ought to match the general shape and timescale of Ediacaran–Cambrian carbon isotopic excursions, if the carbon cycles are, in fact, genetically linked to an oceanographic legacy of type II TPW.

5.14.4 Critical Testing of Cryogenian–Cambrian TPW

5.14.4.1 Ediacaran–Cambrian TPW: 'Spinner Diagrams' in the TPW Reference Frame

While Kirschvink *et al.* (1997) suggested that a single TPW event in the interval ~530–508 Ma accounted for the anomalous dispersion between Late Neoproterozoic and Late Cambrian poles for most continents, Evans and Kirschvink (1999); adopted by Kirschvink and Raub (2003) noted that, in fact, straightforward interpretation of the time-series order of dispersed poles for relatively well-constrained continents like Australia demands multiple TPW events.

Although none of the Cryogenian–Cambrian paleomagnetic poles for Australia is 'absolutely' dated, stratigraphic order between those poles is clear; many come from a single sedimentary succession (South Australia's Adelaide 'geosyncline').

We prefer a terminal Cryogenian–Ediacaran–Cambrian APWP for Australia composed of the poles in **Table 1**. While these poles are of varying quality, none can be demonstrated persuasively to have been remagnetized, or to have dramatically wrong age assignments without basing such an argument on the inexplicability of the magnetization direction itself. Many other paleomagnetic poles for Australia in this time interval have been excluded from our analysis, using data selection and supercedence criteria we believe uncontroversial, but beyond the scope of this chapter.

The oldest group of poles, uppermost 'Cryogenian' in age, are probably ~635 Ma or slightly older, based on 'Snowball Earth' lithological and chemostratigraphic correlation to well-dated successions in Namibia and South China. Four published poles from the Elatina Formation and one from the immediately underlying Yaltipena Formation, presumed genetically related to the onset of Elatina glaciation or deglaciation, cluster well, placing Australia very near the equator. (In today's geomagnetic reference frame, paleopole longitudes for this cluster are near 330, 360 °E and pole latitudes are in 40, 55 °S.) A pole position from immediately overlying, earliest Ediacaran Brachina Formation siliciclastics, is similar though slightly far-sided.

The only Mid-Ediacaran paleomagnetic pole we consider is that of the undated Bunyeroo Formation, ~200–400 m stratigraphically higher, and separated from uppermost Brachina Formation by at least one supersequence boundary in those study areas of South Australia. Although the Bunyeroo Formation is lithologically similar to the Brachina Formation, shares a similar burial and gentle-folding tectonic history, and passes a reliability-by-comparison test with the Acraman Impact meltrock aeromagnetic anomaly on the nearby Gawler Craton (the Bunyeroo Formation hosts ejecta of that impact event), its pole position is significantly different, lying at 16.3° E, −18.1° S (Schmidt and Williams, 1996), and implying mostly counterclockwise rotation of Australia, in the celestial reference frame, during Early Ediacaran time.

Kirschvink's (1978) middle-upper Ediacaran pole from central Australia's Upper Pertatataka Formation and Lower Arumbera Formation returns to the vicinity of Elatina poles, suggesting mid-Ediacaran clockwise rotation for Australia in the celestial reference frame. Terminal Ediacaran magnetization from upper Arumbera Formation is broadly similar.

Lower Cambrian poles from South Australia once more return to the vicinity of 340, 015 °E and ~−45 °S, suggesting terminal Ediacaran or earliest

Table 1 Paleomagnetic poles defining 'Cryogenian'–Ediacaran–Cambrian APW oscillations for Australia

Pole #	Pole ID	Site latitude	Site longitude	Pole latitude	Pole longitude	dp	dm	Age order (1 = oldest)	Reference
14	Hudson	−17	129	18	19	13	13	9	Luck (1972)
13	Hugh River	−23.8	133	11.2	37.2	4.9	9.4	8	Embleton (1972)
12	Billy Creek[a]	−31.1	138.7	−37.4	20.1	7.2	14.4	7	Klootwijk (1980)
11	Kangaroo Isl. A	−35.6	137.6	−33.8	15.1	6.2	12.3	7	Klootwijk (1980)
10	Todd River/ Allua/Eninta	−23.4	133.4	−43.2	339.9	4.5	7.7	7	Kirschvink (1978)
9	Upper Arumbera	−23.4	133.4	−46.6	337.4	2.6	4.6	6	Kirschvink (1978)
8	Lower Arumbera/ upper Pertatataka	−23.4	133.4	−44.3	341.9	7.7	13.6	5	Kirschvink (1978)
7	Bunyeroo	−31.6	138.6	−18.1	16.3	6.5	11.8	4	Schmidt and Williams (1996)
6	Brachina	−30.5	139	−33	328	12	20	3	McWilliams and McElhinny (1980)
5	Elatina SKCB	−31.3	138.7	−39.6	1.7	3.3	6.4	2	Sohl *et al.* (1999)
4	Elatina SW	−31.2	138.7	−51.5	346.6	7.7	15.3	2	Schmidt and Williams (1995)
3	Elatina SWE	−32.4	138	−54.3	326.9	0.9	1.8	2	Schmidt, Williams, and Embleton (1991)
2	Elatina EW	−32.4	138	−51.1	337.1	1.7	3.4	2	Embleton and Williams (1986)
1	Yaltipena	−31.3	138.7	−44.2	352.8	5.8	11.3	1	Sohl *et al.* (1999)
	best-fit great circle			114.3	−32.2				

[a]Billy Creek result is excluded from swath-pole statistics by preference for possibly coeval 'Kangaroo Island A' result; but listed here to weigh against oroclinal rotation between distant Flinders Ranges sites as an alternative explanation for pole dispersion.

Cambrian counterclockwise rotation of Australia, and Cambro-Ordovician paleopoles from South, central, and northern Australia all are still further shifted northward in the modern reference frame, permitting one long Ediacaran–Cambrian TPW event (per Kirschvink *et al.*, 1997) or multiple events of unresolved duration and magnitude summing to the same net rotation.

The resulting Australian APWP (**Figure 9(a)**) does not resemble a time-progressive 'path' so much as a pole 'swath' (although in fact, time progression of that path would indicate repeated reversal of rotational motion for Australia in the celestial reference frame).

We suggest that a more insightful way to view such an APW swath is in the hypothesized TPW reference frame itself. We calculate a best-fit great circle to Australia's APW swath using modified least-squares techniques; in so doing, we assume that (multiple) TPW over the time interval spanned by the constituent poles occurred at a rate far greater than Australia's tectonic-plate motion in the deep-mantle reference frame. This best-fitting great circle, and its corresponding pole with 95% confidence, are shown in **Figure 9(b)**.

By rotating Australia and its pole swath and best-fitting great circle so that the pole to that circle is at the center of an equal-area projection, we place the hypothesized TPW axis at the 'pole' of the stereonet. If TPW were sufficiently fast, and since polarity choice of each paleopole is arbitrary, Australia may

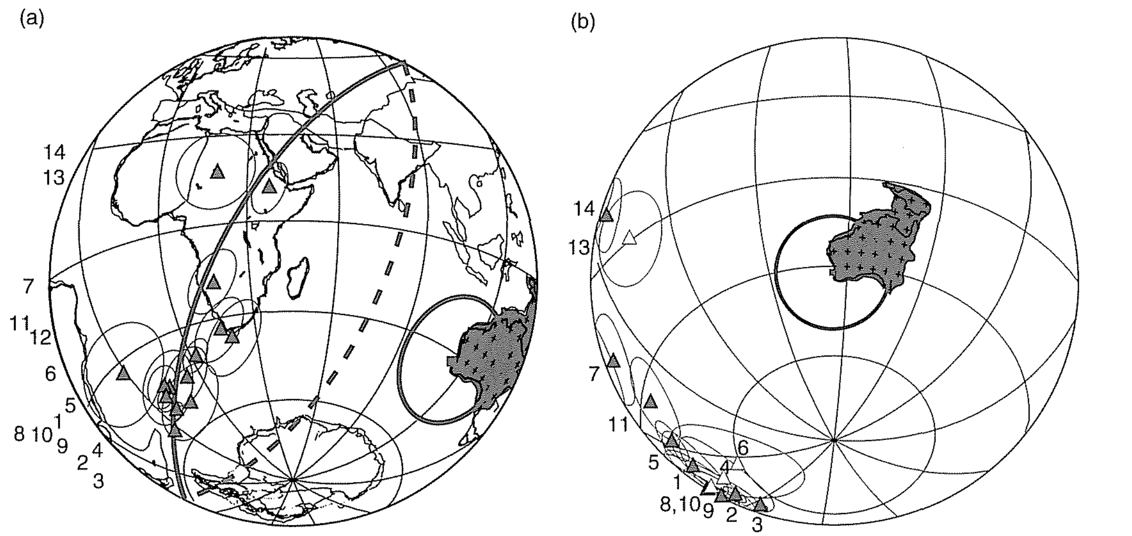

Figure 9 Example of a 'spinner diagram'. (a) Late Cryogenian–Ediacaran–Cambrian APW swath for Australia in the modern geographic reference frame. Fourteen critical poles, dated by biostratigraphy or relative stratigraphic position, appear widely dispersed, and the pole (with 95% confidence trace) to a great circle best-fitting thirteen of those poles lies near the western margin of the Australian Craton. (b) Rotation of Australia, its APW swath, and the swath's best-fitting great circle so that the pole to that swath lies at the center of an equal-area projection creating a 'spinner diagram'. If it is supposed that the back-and-forth time series comprising a continent's APW swath represents multiple (type II) TPW events at rates substantially faster than (or parallel to) plate motion; and if it is assumed, by reasoning outlined in the text and in Kirschvink *et al.* (1997) and Evans (1998, 2003) that the TPW axis lies on Earth's spin-equator, then because of geomagnetic polarity ambiguity in Neoproterozoic time, Australia's actual geographic location at most times during the interval spanning all proposed TPW events may be any rotationally equivalent location that preserves coincidence of its APW swath pole and the TPW axis. For the purposes of paleogeographic reconstruction, Australia's geomagnetic (= rotational) paleolatitude is constrained only for the discrete times of direct paleomagnetic constraints as represented by the individual poles. If rapid type II TPW oscillations were occurring on timescales of a few million years or less, then traditional comparisons of separate plates' paleolatitudes would be meaningless except in the rare instance of extremely precise agreement in pole ages from those plates. Each point on the Earth does, however, maintain a constant angular distance from a type II TPW axis, thus continents can be reconstructed relative to that reference frame. In practical terms from the figured example, Australia may be 'spun' around the (constantly equatorial) TPW axis shown in the center of the diagram. An alternative set of paleogeographic positions occupies the far hemisphere about the antipole to the TPW axis.

effectively occupy any rotationally identical position about that TPW axis, except for precise ages where its paleolatitude is constrained by a corresponding pole. (At those ages, Australia may occupy one of precisely two absolute paleogeographic positions, in the TPW reference frame, recognizing geomagnetic polarity ambiguity).

At all other times, there is rotational paleolatitude ambiguity associated with rapid oscillations about the TPW reference axis. We call this projection a 'spinner' diagram, because the position of a continental block may be freely 'spun' about the TPW axis at the center of the spinner projection. Since all continents must undergo identical TPW, all continental blocks' computed spinner diagrams may be overlapped; and each continent 'spun' to avoid overlaps, to produce a permissible intercontinental paleogeography in the TPW reference frame.

5.14.4.2 Proof of Concept: Independent Reconstruction of Gondwanaland Using Spinner Diagrams

Although Australia's paleomagnetic APW swath is by far the best constrained of the Gondwanaland-constituent continents, all those Gondwanaland elements show dispersed paleopoles easily fit by great circles. We show those APW swaths for India and Antarctica (Mawsonland), for 'Arabia(-Nubia)', for all of 'Africa' (assuming Congo–Kalahari coherence and ignoring pole-less Sao Francisco), and for all of 'South America' (assuming Amazonia–Rio de la Plata coherence). These swaths are depicted in **Figure 10** using poles in **Table 2**, in both the present geomagnetic reference frame and as spinner diagrams in the inferred TPW reference frame.

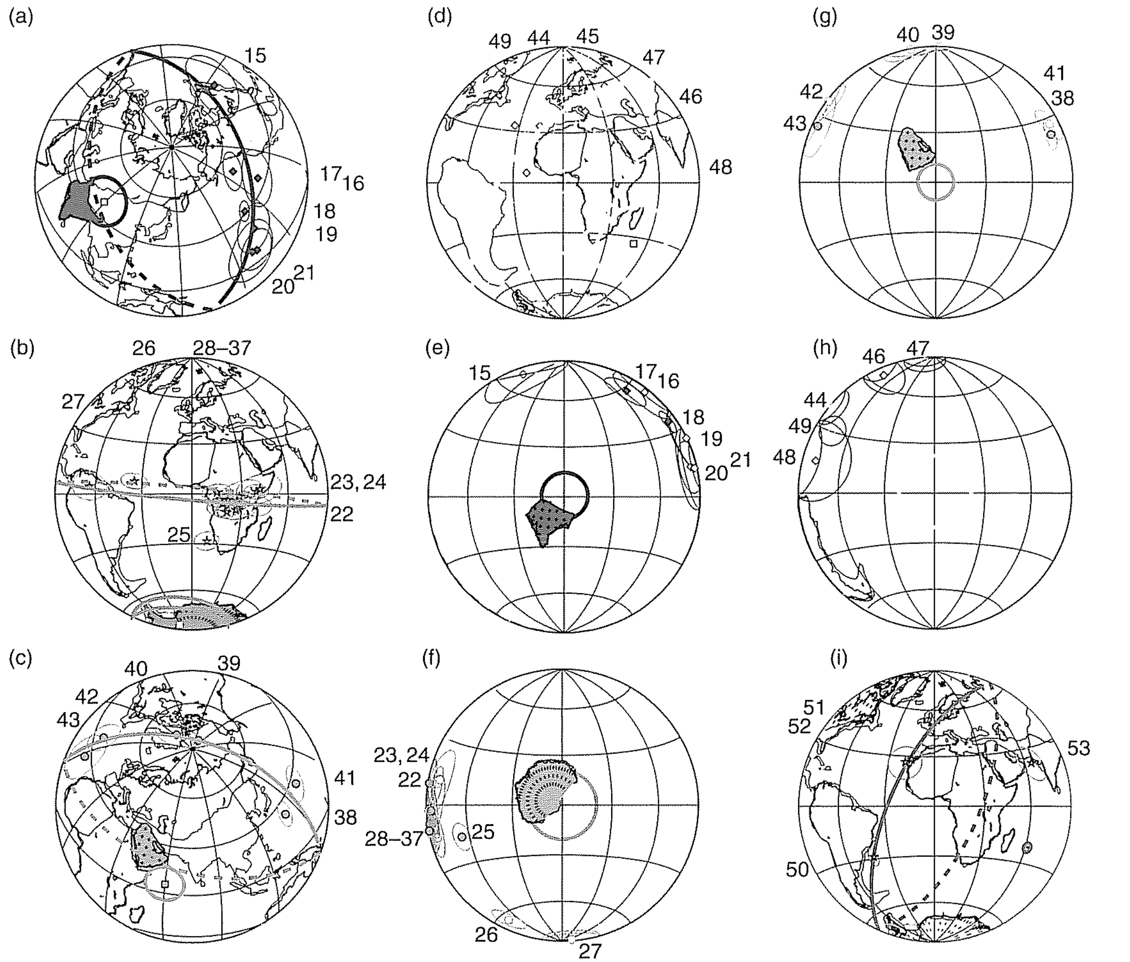

Figure 10 Elaboration of proto-Gondwanaland's APW commonality. Late Cryogenian–Ediacaran–Cambrian APW distributions, in the modern geographic reference frame (but various views) for the Indian and Antarctic Cratons; for 'Arabia', a simplification of the Arabian-Nubian shield and Neoproterozoic basement in modern Iran; for 'South America', a simplification of the Neoproterozoic Rio de la Plata and Amazonia Cratons in late Brasiliano time; and for 'Africa', a simplification of the Neoproterozoic Kalahari and Congo–Sao Francisco Cratons (see text for tectonic reconstruction caveats). All cratons except 'Africa' are also represented in spinner diagrams using poles to best-fitting great circles through critical-pole APW distributions. Adapted from figure 3 in Evans DA, *et al.* (1998) Polar wander and the Cambrian. *Science* 279: 9a–9e.

We are favorably impressed that, by superimposing each continent's APW swath pole at the center of a common spinner projection, continents may be 'spun' so that a nearly Gondwanaland configuration is produced, with relatively minor shifting of each continent's APW swath pole within its 95% confidence limit (**Figure 11**).

Although we recognize that Gondwanaland was not yet entirely formed during Ediacaran–Cambrian time (e.g., Boger *et al.*, 2001; Collins and Pisarevsky, 2005; Valeriano *et al.*, 2004), the post-Ediacaran relative movements between its constituents should have been minor, and even Late-Precambrian stitching of constituent African and South American Cratons was permissibly nonmobilistic on a tens of degrees spatial scale (Veevers, 2004). We also recognize that our Arabia-Nubia 'craton' includes amalgamated terranes and basement of varying age (Veevers, 2004); therefore, our tectonic definition of 'Gondwanaland', and its implied inheritance from latest Neoproterozoic Rodinia fragmentation, is first-order only.

Nonetheless, this reconstruction restores Gondwanaland to a configuration resembling that calculated by back-rotating post-Pangean seafloor spreading ridges by an entirely independent method, predicated only on the assumption that Late Neoproterozoic–Early Cambrian TPW was

Table 2 Paleomagnetic poles defining 'Cryogenian'–Ediacaran–Cambrian APW oscillations for other Gondwanaland constituents

Pole #	Pole ID	Site Latitude	Site longitude	Pole latitude	Pole longitude	dp	dm	Age order (1 = oldest)	Reference
	India			89.3	38.3	13.8	13.8		
21	Salt Range pseudomorph rot. 30°	32.7	73	7.2	192	9	11.8	6	Wenski, 1972
20	Purple sandstone rot. 30°	32.7	73	8.2	189.4	12.5	18.5	5	McElhinny, 1970
19	Khewra A rot. 30°	32.3	71	19.3	197	10	14	4	Klootwijk *et al.*, 1986
18	Bhander sandstone	23.7	79.6	31.5	199	3.1	5.9	3	Athavale *et al.*, 1972
17	Upper Vindhyan Rewa-Bhander	27	77.5	51	217.8	5.6	11.2	2.5	McElhinny, 1970
16	Rewa	23.8	78.9	35	222	9.6	15.9	2	Athavale *et al.*, 1972
15	Mundwarra Complex	25	73	42	295	12	22	1	Athavale *et al.*, 1963
	Antarctica (Mawsonland)			234.8	−83.5				
37	Teall Nunatak	−74.9	162.8	−11	31	3.6	7.2	8	Lanza and Tonarini, 1998
36	Wright Valley granitics	−77.5	161.6	−5.5	18.4	4.1	8.2	8	Funaki, 1984
35	Lake Vanda feldspar porphyry dikes	−77.5	161.7	−4	27	4.3	8.6	7	Grunow, 1995
34	Dry Valley mafic swarm	−77.6	163.4	−9.4	26.7	5.5	10.9	7	Manzoni and Nanni, 1977
33	Killer Ridge Mt. Loke diorites	−77.4	162.4	−7.1	21.2	6	12	6	Grunow and Encarnacion, 2000
32	Lake Vanda Bonny pluton	−77.5	161.7	−8.3	27.8	6.6	13.1	6	Grunow, 1995
31	Granite Harbour pink granite	−76.8	162.8	−3.4	16.6	4.4	8.5	6	Grunow, 1995
30	Granite Harbour mafic dikes	−77	162.5	0.9	15	4.7	9	6	Grunow, 1995
29	Granite Harbour grey granite	−77	162.6	−3.6	21.7	3.3	6.5	6	Grunow, 1995
28	Mirnyy Station charnokites	−66.5	93	−1.4	28.6	8	16	5	McQueen *et al.*, 1972
27	Upper Heritage Group	−79.2	274	4	296	7.1	12.5	5	Watts and Bramall, 1981
26	Liberty Hills Formation	−80.1	276.9	7.3	325.4	4.3	8.6	4	Randall *et al.*, 2000
25	Sor Rondane intrusions	−72	24	−28.4	9.5	9.9	5.7	3	Zijderveld, 1968
24	Briggs Hill Bonny pluton	−77.8	163	2.7	41.4	7.8	15	2	Grunow, 1995
23	Wyatt Ackerman Mt. Paine tonalite	−86.5	170	1.1	39.3	4	8	1	Grunow and Encarnacion, 2000
22	Zanuck granite	−86.5	38.8	−7.1	38.8	5.5	10.9	1	Grunow and Encarnacion, 2000
	Arabia			60	5.8				
43	Hornblende diorite porphyry	21.7	43.7	25.8	332.2	9.1	14.7	Unknown	Kellogg and Beckmann, 1982
42	Red sandstone, Jordan	29.7	35.3	36.7	323.4	6.7	10	5	Burek, 1968
41	Jorden dikes	29.5	35.1	26	161	5.1	9.4	4	Sallomy and Krs, 1980
40	Arfan/Jujuq	21.3	43.7	77.4	297.9	6.9	12.2	3	Kellogg and Beckmann, 1982
39	Mt. Timna	29.8	34.9	83.6	223.2	3.3	5.4	2	Marco *et al.*, 1993

(*Continued*)

Table 2 (Continued)

Pole #	Pole ID	Site Latitude	Site longitude	Pole latitude	Pole longitude	dp	dm	Age order (1 = oldest)	Reference
38	Mirbat sandstone	17.1	54.8	23.3	141.8	3.9	7.5	1	Kempf *et al.*, 2000
	'South America' (Rio de la Plata, Amazonia, late Brasiliano)			48.5	−34.3				
49	Mirassol d'Oeste remagnetization	−15	302	33.6	326.9	7.1	10	6	Trindade *et al.* (2003)
48	Upper Sierra de las Animas	−34.7	304.7	5.9	338.1	19.6	26.7	5	Sanchez-Bettucci and Rapalini (2002)
47	Campo Alegra	−26.5	310.6	57	43	9	9	4	D'Agrella-Filho and Pacca (1988)
46	Playa Hermosa	−34.7	304.7	43	18.4	8.6	16	3	Sanchez-Bettucci and Rapalini (2002)
45	Mirassol d'Oeste characteristic[a]	15	302	82.6	112.6	5.6	9.3	2	Trindade *et al.* (2003)
44	Urucum	−19	302	34	344	9	9	1	Creer (1965)
	'Africa' (Congo and Kalahari)			61.5	−21.4				
53	Doornport[b]	−23.7	17.2	21.8	64.9	6.8	11	4	Piper (1975)
52	Dedza Mtn. syenite	−14.4	34.3	26	341	10	10	3	McElhinny *et al.* (1968)
51	Ntonya ring structure	−15.5	35.3	27.8	344.9	1.4	2.3	2	Briden *et al.* (1993)
50	Sinyai	0.5	37.1	−29	319	3	5	1	Meert and van der Voo (1996)

[a]The Mirassol ChRM pole falls considerably off of the great circle defined by the younger five South America poles. Following Valeriano *et al.* (2004) we suppose that Mirassol d'Oeste characteristic as an old pole located near a border of the mobile belt, might be rotated. The 'South American' great circle including Mirassol d'Oeste characteristic has a pole at (19.7, 242.9).

[b]Doornport, a likely Cambrian remagnetization, is internal to the Damaride fold belt. It is far from the (admittedly underconstrained) 'African' great circle that it must either indicate inappropriate lumping of date from the constituent cratons, or else it has been rotated by Damaride structures. We acknowledge the relatively unsatisfying character of the 'African' and 'South American' databases, but leave full consideration for a future paper.

Neither 'South America' nor 'Africa' existed in any semblence of the modern, during 'Cryogenian' – Ediacaran – Cambrian time. However, the 'constituent' Precambrian cratons of each – Rio de la Plata and Amazonia for South America; and Kalahari and Congo–Sao Francisco for Africa, might have remained nearly fixed with respect to each other during pan-Africal and Brasiliano mobilism. Likewise, although the 'Arabian-Nubian' shield incorporates significant juvenile arc material, we suppose it might have occupied a common general area of latest Neoproterozoic real estate, including basement terranes. In any case, it is intriguing that, as a 'block,' Arabia may be treated, essentially, as one of the other cratons, by owning a dispersed APW swat which, when fit to a great circle, reconstructs nearly to Gondwanaland configuration independent of seafloor retro-rotations.

We consider it almost certain that some of these paleomagnetic poles, unconstrained by direct field tests of magnetization fidelity, are in fact remagnetizations or tectonically rotated. However we have attempted to compile a list of possibly primary magnetizations which could not be discounted except by concern for the actual direction obtained.

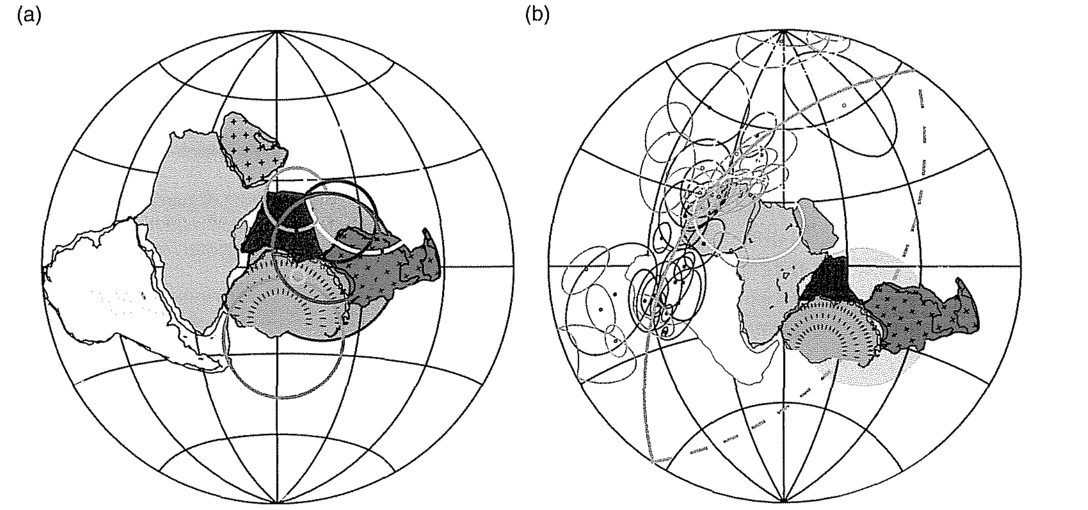

Figure 11 Multiple type II TPW in Late Cryogenian–Ediacaran–Cambrian time, proof of concept. (a) Using only spinner diagrams, spinning each continent about its own APW swath-fitting great-circle pole, and shifting those poles about a common, inferred TPW axis within each 95% confidence limit, it is possible to reconstruct Gondwanaland approximately. Because Gondwanaland formed during the same period of time as these hypothesized multiple TPW events, with possibly minor reshuffling of the constituent Rodinia Cratons, we expect its later-dispersed fragments to share the essentially common APW swath shown in (b). This is equivalent to the earliest APW swings depicted by Evans (2003; **figure 3**) using the same logic, and it expands upon the pole database of Kirschvink *et al.* (1997). Any alternative interpretation to the hypothesis of multiple, rapid type II TPW events for Late Neoproterozoic to Cambrian time must explain not only the individual, dispersed poles and continental APWPs, it must also explain why all of the constituent cratons of Gondwanaland show APWPs which are of differing sense in the modern geographic reference frame, but which restore to near-coincidence when viewed in the Gondwanaland reference frame.

multiple and rapid relative to the rates of plate motion. We consider this proof of concept that the Ediacaran–Cambrian multiple TPW hypothesis is a viable, non-trivially discounted explanation for general dispersion of paleomagnetic poles of that age.

5.14.5 Summary: Major Unresolved Issues and Future Work

Although little-metamorphosed Precambrian rocks exist and may hold primary magnetization with equal fidelity to unmetamorphosed Phanerozoic rocks, the ancient paleomagnetic database is severely underconstrained, both spatially and temporally. We consider it equally likely that better pan-continental paleomagnetic coverage of TPW intervals already hypothesized will offer non-TPW alternatives for those events, and that more detailed geographic and temporal APW determinations will recognize many new apparent TPW events.

For continental reconstructions of any age, quick and/or repeated, oscillatory type II TPW will be resolved better by detailed magnetostratigraphy of thick, continuous-deposited volcanic or sedimentary successions. Relatively few such magnetostratigraphies exist, even through Paleozoic and Mesozoic time.

Geodynamic modeling of TPW should address the predicted effects of multiple and/or quick (type II) TPW events, as well as longer-duration, large-magnitude (type I) TPW events. We have not yet been able to satisfactorily fathom the dynamics of viscoelastic relaxation by a highly viscosity-structured mantle, if those dynamics in fact have been addressed in the geophysical literature.

Although mantle-driven TPW seems to predict (and even partly rely upon) dynamic topography, we understand that it is not clear that any modern-day surface physiographic feature is unambiguously isostatically uncompensated. We hope that this paradox will trigger additional work and debate in the near future.

If multiple, fast Ediacaran–Cambrian TPW events are not borne out by future, detailed magnetostratigraphic investigation, we will be fascinated to discover the otherwise incredible misfortune explaining the distribution of the dispersed APW swaths that today rotate those hypothesized TPW events into coincidence with the same parameters which reconstruct Gondwanaland in the Mesozoic Era.

Sequence-stratigraphic compilations for times of hypothesized TPW should show global quadrature, rather than global constructive synchroneity, when paleolatitudes of those deposits are considered in a spinner-diagram-derived global paleogeography.

Physical and chemical oceanographic changes predicted by TPW should be observed in the rock record synchronous with hypothesized or demonstrated TPW of sufficient magnitude; and some of these predictions (e.g., atmospheric temperature anomaly resulting from methane clathrate destabilization) should be testable by independent methods, where the rock record is amenable.

Acknowledgments

The authors are grateful for comments and criticisms from Dennis Kent, Bob Kopp, Adam Maloof, Ross Mitchell, and Will Sager. Adam Maloof developed spinner diagrams in concert with TDR and DADE. Jean-Pascal Cogne's *Paleomac*© program (downloaded with password permission from J-PC) readily produces spinner diagrams. This work is supported in part by a 3-year NSF Graduate Fellowship to TDR, NSF grants 9807741, 9814608, and 9725577 and funds from the NASA National Astrobiology Institute to JLK, and a David and Lucile Packard Foundation Award to DADE.

References

Alvarez W, *et al.* (1977) Upper Cretaceous–Paleocene magnetic stratigraphy at Gubbio, Italy. Part 5: Type Section for Late Cretaceous–Paleocene geomagnetic reversal time scale. *Geological Society of America Bulletin* 88(3): 383–388.

Alvarez W and Lowrie W (1978) Upper Cretaceous paleomagnetic stratigraphy at Moria (Umbrian Apennines, Italy) – Verification of Gubbio section. *Geophysical Journal of the Royal Astronomical Society* 55(1): 1–17.

Anderson DL (1982) Hotspots, polar wander, Mesozoic convection and the geoid. *Nature* 297: 391–393.

Anderson DL (1990) *Theory of the Earth*, 366 pp. Boston, MA. Blackwell Scientific Publications.

Anderson DL (1994) Superplumes or Supercontinents *Geology* 22(1): 39–42.

Andrews DL, *et al.* (2006) Uncertainties in plate reconstructions relative to the hotspots; Pacific-hotspot rotations and uncertainties for the past 68 million years. *Geophysical Journal International* 166(2): 939–951.

Athavale RN, *et al.* (1963) Paleomagnetism of some Indian Rocks. *Geophysical Journal of the Royal Astronomical Society* 7(3): 304–313.

Athavale RN, *et al.* (1972) Paleomagnetism and age of Bhader and Rewa sandstones from India. *Geophysical Journal of the Royal Astronomical Society* 28(5): 499–509.

Beck ME and Housen BA (2003) Absolute velocity of North America during the Mesozoic from paleomagnetic data. *Tectonophysics* 377(1-2): 33–54.

Besse J and Courtillot V (1991) Revised and synthetic apparent polar wander paths of the African, Eurasian, North-American and Indian Plates, and true polar wander since 200 Ma. *Journal of Geophysical Research-Solid Earth and Planets* 96(B3): 4029–4050.

Besse J and Courtillot V (2002) Apparent and true polar wander and the geometry of the geomagnetic field over the last 200 Myr. *Journal of Geophysical Research-Solid Earth* 107(B11).

Besse J and Courtillot V (2003) Apparent and true polar wander and the geometry of the geomagnetic field over the last 200 Myr (vol 107, art no 2300, 2002). *Journal of Geophysical Research-Solid Earth* 108(B10).

Biram J (1966) *A. Wegener: The Origin of Continents and Oceans 4th edn. New York, NY: Dover Publications.*

Boger SD, *et al.* (2001) Early Paleozoic tectonism within the east Antarctic craton: The final suture between east and west Gondwana?. *Geology* 29(5): 463–466.

Brasier MD, *et al.* (1994) Multiple delta-13C excursions spanning the Cambrian explosion to the Botomian crisis in Siberia. *Geology* 22(5): 455–458.

Buffett B and Archer D (2004) Global inventory of methane clathrate: Sensitivity to changes in the deep ocean. *Earth and Planetary Science Letters* 227(3-4): 185–199.

Camps P, *et al.* (2002) Comment on 'Stability of the Earth with respect to the spin axis for the last 130 million years' by JA. Tarduno and A.Y. Smirnov (2001) [*Earth and Planetary Science Letters* 184: 549–553] *Earth and Planetary Science Letters*198(3-4): 529–532.

Celaya MA, *et al.* (1999) Climate-driven polar motion. *Journal of Geophysical Research Solid Earth* 104(B6): 12813–12829.

Chase CG and Sprowl DR (1983) The modern geoid and ancient plate boundaries. *Earth and Planetary Science Letters* 62(3): 314–320.

Collins AS and Pisarevsky SA (2005) Amalgamating eastern Gondwana: The evolution of the Circum-Indian orogens. *Earth-Science Reviews* 71(3-4): 229–270.

Cottrell RD and Tarduno JA (2000) Late Cretaceous true polar wander: Not so fast. *Science* 288: 2283a.

Cottrell RD and Tarduno JA (2003) A Late Cretaceous pole for the Pacific plate: Implications for apparent and true polar wander and the drift of hotspots. *Tectonophysics* 362(1-4): 321–333.

Darwin G (1877) On the influence of geological changes on the Earth's axis of rotation. *Philosophical Transactions of the Royal Society of London* 167: 271–312.

Davies GF (1984) Lagging mantle convection, the geoid and mantle structure. *Earth and Planetary Science Letters* 69(1): 187–194.

Dickens GR, *et al.* (1995) Dissociation of oceanic methane hydrate as a cause of the carbon-isotope excursion at the end of the Paleocene. *Paleoceanography* 10(6): 965–971.

Dickens GR, *et al.* (1997) A blast of gas in the latest Paleocene: Simulating first-order effects of massive dissociation of oceanic methane hydrate. *Geology* 25(3): 259–262.

Dickman SR (1979) Continental-drift and true polar wandering. *Geophysical Journal of the Royal Astronomical Society* 57(1): 41–50.

DiVenere V and Kent DV (1999) Are the Pacific and Indo-Atlantic hotspots fixed? Testing the plate circuit through Antarctica. *Earth and Planetary Science Letters* 170(1-2): 105–117.

DuBois PM (1957) Comparison of palaeomagnetic results from selected rocks of Great Britain and North America. *Philosophical Magazine Supplement Advances in Physics* 6: 177.

Elkins-Tanton LT and Hager BH (2005) Giant meteoroid impacts can cause volcanism. *Earth and Planetary Science Letters* 239(3-4): 219–232.
Evans DA, *et al.* (1998) Polar wander and the Cambrian. *Science* 279: 9a–9e.
Evans DAD and Kirschvink JL (1999) Multiple episodes of rapid true polar wander in Neoproterozoic–Cambrian time?, paper presented at Geological Society of America Annual meeting, Geological Society of America (GSA). Boulder, CO.
Evans DAD (2003) True polar wander and supercontinents. *Tectonophysics* 362(1-4): 303–320.
Evans DAD (2006) Proterozoic low orbital obliquity and axial-dipolar geomagnetic field from evaporite palaeolatitudes. *Nature* 444(7115): 51–55.
Evans DAD, *et al.* (2000) A high-quality mid-Neoproterozoic paleomagnetic pole from south China, with implications for ice ages and the breakup configuration of Rodinia. *Precambrian Research* 100(1-3): 313–334.
Evans ME (1976) Test of dipolar nature of geomagnetic field throughout Phanerozoic time. *Nature* 262(5570): 676–677.
Evans ME (2005) Testing the geomagnetic dipole hypothesis: Palaeolatitudes sampled by large continents. *Geophysical Journal International* 161(2): 266–267.
Farley KA and Eltgroth SF (2003) An alternative age model for the Paleocene-Eocene thermal maximum using extraterrestrial He-3. *Earth and Planetary Science Letters* 208(3-4): 135–148.
Fisher D (1974) Some more remarks on polar wandering. *Journal of Geophysical Research* 79(26): 4041–4045.
Fujita M, *et al.* (2002) Oceanic torques on solid Earth and their effects on Earth rotation. *Journal of Geophysical Research-Solid Earth* 107(B8).
Funaki M (1984) Investigation of the Paleomagnetism of the basement-complex of Wright Valley, southern Victoria Land, Antarctica. *Journal of Geomagnetism and Geoelectricity* 36(11): 529–563.
Gold T (1955) Instability of the Earth's axis of rotation. *Nature* 175: 526–529.
Goldreich P and Toomre A (1969) Some remarks on polar wandering. *Journal of Geophysical Research* 74(10): 2555–2567.
Gordon RG, *et al.* (1984) Paleomagnetic Euler Poles and the apparent polar wander and absolute motion of North-America since the Carboniferous. *Tectonics* 3(5): 499–537.
Gordon RG (1987) Polar wandering and paleomagnetism. *Annual Review of Earth and Planetary Sciences* 15: 567–593.
Gordon RG (1995) Plate motions, crustal and lithospheric mobility, and paleomagnetism: Prospective viewpoint. *Journal of Geophysical Research,Solid Earth* 100(B12): 24367–24392.
Grunow AM (1995) Implications for Gondwana of new Ordovician Paleomagnetic data from Igneous rocks in Southern Victoria Land, East Antarctica. *Journal of Geophysical Research,Solid Earth* 100(B7): 12589–12603.
Grunow AM and Encarnacion JP (2000) Cambro-Ordovician palaeomagnetic and geochronologic data from southern Victoria Land, Antarctica: Revision of the Gondwana apparent polar wander path. *Geophysical Journal International* 141(2): 391–400.
Hager BH, *et al.* (1985) Lower mantle heterogenity, dynamic topography and the geoid. *Nature* 313(6003): 541–546.
Halverson GP, *et al.* (2002) A major perturbation of the carbon cycle before the Ghaub glaciation (Neoproterozoic) in Namibia: Prelude to snowball Earth? *Geochemistry, Geophysics and Geosystems* 3.
Halverson GP, *et al.* (2005) Toward a Neoproterozoic composite carbon-isotope record. *Geological Society of America Bulletin* 117(9–10): 1181–1207.
Harrison CGA and Lindh T (1982) Comparison Between the Hot Spot and Geomagnetic-Field Reference Frames. *Nature* 300(5889): 251–252.
Higgins JA and Schrag DP (2006) Beyond methane: Towards a theory for the Paleocene-Eocene Thermal Maximum. *Earth and Planetary Science Letters* 245(3–4): 523–537.
Higgins MD (2005) A new model for the structure of the Sept Iles Intrusive suite, Canada. *Lithos* 83: 199–213.
Hynes A (1990) 2-Stage Rifting of Pangea by 2 different mechanisms. *Geology* 18(4): 323–326.
Irving E (1956) Palaeomagnetic and paleoclimatological aspects of polar wandering. *Geofisica Pura et Applicata* 33: 23–41.
Irving E (1957) Rock magnetism; a new approach to some palaeogeographic problems. *Advances in Physics* 6(22): 194–218.
Irving E (1988) Paleomagnetic confirmation of Continental Drift. *EOS, Transactions of American Geophysical Union* 69(44): 994–1014.
Irving E (2005) The role of latitude in mobilism debates. *Proceedings of the National Academy of Sciences of the United States of America* 102(6): 1821–1828.
Irving E and Irving GA (1982) Apparent polar wander paths carboniferous through cenozoic and the assembly of Gondwana. *Geophysical Surveys* 5(2): 141–188.
Jurdy DM and Van der Voo R (1974) Method for separation of true polar wander and continental-drift, including results for last 55 my. *Journal of Geophysical Research* 79(20): 2945–2952.
Jurdy DM and Van der Voo R (1975) True polar wander since early cretaceous. *Science* 187(4182): 1193–1196.
Kent DV and Smethurst MA (1998) Shallow bias of paleomagnetic inclinations in the Paleozoic and Precambrian. *Earth and Planetary Science Letters* 160(3–4): 391–402.
Kirschvink JL (1978) Precambrian-Cambrian boundary problem - Paleomagnetic directions from Amadeus Basin, Central Australia. *Earth and Planetary Science Letters* 40(1): 91–100.
Kirschvink JL, *et al.* (1991) The Precambrian-Cambrian boundary: Magnetostratigraphy and Carbon Isotopes resolve correlation problems between Siberia, Morocco, and South China. *GSA Today* 1: 69–91.
Kirschvink JL, *et al.* (1997) Evidence for a large-scale Early Cambrian reorganization of continental masses by inertial interchange true polar wander. *Science* 277: 541–545.
Kirschvink JL, et al. (2005) Rapid inertial-interchange true polar wander during ediacaran time induced by intrusion of the sept-îles intrusive suite, Quebec, Canada: A possible trigger for massive sea-level and carbon isotopic excursions, paper presented at Gondwana XII, Mendoza, Argentina.
Kirschvink JL and Raub TD (2003) A methane fuse for the Cambrian explosion: Carbon cycles and true polar wander. *Comptes Rendus Geoscience* 335(1): 65–78.
Klootwijk CT, *et al.* (1986a) Paleomagnetic constraints on formation of the Mianwali Reentrant, Trans-Indus and Western Salt-Range, Pakistan. *Earth and Planetary Science Letters* 80(3–4): 394–414.
Klootwijk CT, *et al.* (1986b) Rotational overthrusting of the northwestern Himalaya – Further paleomagnetic evidence from the Riasi thrust sheet, Jammu foothills, India. *Earth and Planetary Science Letteres* 80(3-4): 375–393.
Lanza R and Tonarini S (1998) Palaeomagnetic and geochronological results from the Cambro-Ordovician granite harbour intrusives inland of Terra Nova Bay (Victoria Land, Antarctica). *Geophysical Journal International* 135(3): 1019–1027.
Li ZX, *et al.* (2004) A 90 degrees spin on Rodinia: Possible causal links between the Neoproterozoic supercontinent, superplume, true polar wander and

low-latitude glaciation. *Earth and Planetary Science Letters* 220(3-4): 409–421.

Llanos MPI, Riccardi AC, and Singer SE (2006) Palaeomagnetic study of Lower Jurassic marine strata from the Neuquen Basin, Argentina: A new Jurassic apparent polar wander path for South America. *Earth and Planetary Science Letters* 252(3–4): 379–397.

Magaritz M, *et al.* (1986) Carbon-isotope events across the Precambrian–Cambrian boundary on the Siberian platform. *Nature* 320: 258–259.

Magaritz M, *et al.* (1991) The Precambrian–Cambrian boundary problem: Carbon isotope correlations for Vendian and Tommotian time between Siberia and Morocco. *Geology* 19: 847–850.

Maloof AC, *et al.* (2005) An expanded record of Early Cambrian carbon cycling from the anti-atlas margin, Morocco. *Canadian Journal of Earth Sciences* 42(12): 2195–2216.

Maloof AC, *et al.* (2006) Combined paleomagnetic, isotopic, and stratigraphic evidence for true polar wander from the Neoproterozoic Akademikerbreen Group, Svalbard, Norway. *Geological Society of America Bulletin* 118(9-10): 1099–1124.

Manzoni M and Nanni T (1977) Paleomagnetism of Ordovician lamprophyres from Taylor Valley, Victoria Land, Antarctica. *Pure and Applied Geophysics* 115(4): 961–977.

Marcano MC, *et al.* (1999) True polar wander during the Permo-Triassic. *Journal of Geodynamics* 28(2-3): 75–95.

Matsuyama I, *et al.* (2006) Rotational stability of dynamic planets with elastic lithospheres. *Journal of Geophysical Research-Planets* 111(E2): E02003.

McQueen DM, *et al.* (1972) Cambro-Ordovician paleomagnetic pole position and rubidium–strontium total rock isochron for charnockitic rocks from Mirnyy Station, east Antarctica. *Earth and Planetary Science Letters* 16(3): 433–438.

Meert JG (1999) A paleomagnetic analysis of Cambrian true polar wander. *Earth and Planetary Science Letters* 168(1-2): 131–144.

Mitrovica JX, *et al.* (2001a) Glacial isostatic adjustment on a rotating Earth. *Geophysical Journal International* 147(3): 562–578.

Mitrovica JX, *et al.* (2001b) Recent mass balance of polar ice sheets inferred from patterns of global sea-level change. *Nature* 409(6823): 1026–1029.

Mitrovica JX, *et al.* (2005) The rotational stability of an ice-age Earth. *Geophysical Journal International* 161(2): 491–506.

Mitrovica JX and Forte AM (2004) A new inference of mantle viscosity based upon joint inversion of convection and glacial isostatic adjustment data. *Earth and Planetary Science Letters* 225(1-2): 177–189.

Montanez IP, *et al.* (2000) Evolution of the Sr and C isotope composition of Cambrian oceans. *GSA Today* 10(5): 1–7.

Moreau M-G, *et al.* (2007) A New global Paleocene–Eocene apparent polar wandering path loop by 'stacking' magnetostratigraphies: Correlations with high latitude climatic data. *Earth and Planetary Science Letters,* doi: 10.1016/j.epsl.2007.05.025.

Mound JE, *et al.* (1999) A sea-level test for inertial interchange true polar wander events. *Geophysical Journal International* 136(3): F5–F10.

Mound JE, *et al.* (2001) Sea-level change and true polar wander during the Late Cretaceous. *Geophysical Research Letters* 28(10): 2057–2060.

Mound JE, *et al.* (2003) The equilibrium form of a rotating Earth with an elastic shell. *Geophysical Journal International* 152(1): 237–241.

Mound JE and Mitrovica JX (1998) True polar wander as a mechanism for second-order sea-level variations. *Science* 279(5350): 534–537.

Muller RD, *et al.* (1993) Revised plate motions relative to the hotspots from combined Atlantic and Indian-Ocean hotspot tracks. *Geology* 21(3): 275–278.

Munk WH and MacDonald GJF (1960) *The Rotation of the Earth.* Cambridge, UK: Cambridge University Press.

Nakada M (2002) Polar wander caused by the Quaternary glacial cycles and fluid Love number. *Earth and Planetary Science Letters* 200(1-2): 159–166.

Nakiboglu SM and Lambeck K (1980) Deglaciation effects on the rotation of the Earth. *Geophysical Journal of the Royal Astronomical Society* 62(1): 49–58.

Nimmo F (2002) Why does Venus lack a magnetic field? *Geology* 30(11): 987–990.

Nimmo F and Pappalardo RT (2006) Diapir-induced reorientation of Saturn's moon Enceladus. *Nature* 441(7093): 614–616.

Payne JL, *et al.* (2004) Large perturbations of the carbon cycle during recovery from the end-Permian extinction. *Science* 305(5683): 506–509.

Peltier WR (1998) Postglacial variations in the level of the sea: Implications for climate dynamics and solid-Earth geophysics. *Reviews of Geophysics* 36(4): 603–689.

Petronotis KE and Gordon RG (1999) A Maastrichtian palaeomagnetic pole for the Pacific plate from a skewness analysis of marine magnetic anomaly 32. *Geophysical Journal International* 139(1): 227–247.

Phillips RJ, *et al.* (2001) Ancient geodynamics and global-scale hydrology on Mars. *Science* 291: 2587–2591.

Piper JDA (2006) A approximate to 90 degrees Late Silurian–Early Devonian apparent polar wander loop: The latest inertial interchange of planet Earth? *Earth and Planetary Science Letters* 250(1-2): 345–357.

Piper JDA and Zhang QR (1999) Palaeomagnetic study of Neoproterozoic glacial rocks of the Yangzi Block: Palaeolatitude and configuration of south China in the Late Proterozoic supercontinent. *Precambrian Research* 94(1-2): 7–10.

Pisarevsky SA, *et al.* (2003) Models of Rodinia assembly and fragmentation. In: Yoshida M, Windley BF, and Dasgupta S (eds.) *Proterozoic East Gondwana: Supercontinent Assembly and Breakup*, pp. 35–55. London: Geological Society of London.

Porco CC, *et al.* (2006) Cassini observes the active south pole of Enceladus. *Science* 311(5766): 1393–1401.

Prevot M, *et al.* (2000) Evidence for a 20 degrees tilting of the Earth's rotation axis 110 million years ago. *Earth and Planetary Science Letters* 179(3-4): 517–528.

Ranalli G (1995) *Rheology of the Earth*, 413 pp. London: Chapman and Hall.

Randall DE, *et al.* (2000) A new Late Middle Cambrian paleomagnetic pole for the Ellsworth Mountains, Antarctica. *Journal of Geology* 108(4): 403–425.

Richards MA, *et al.* (1997) An explanation for Earth's long-term rotational stability. *Science* 275(5298): 372–375.

Richards MA and Engebretson DC (1992) Large-scale mantle convection and the history of subduction. *Nature* 355(6359): 437–440.

Riisager P, Riisager J, Abrahamsen N, and Waagskin R (2002) New Paleomagnetic pole and magnetostratigraphy of Faroe Islands flood volcanics, North Atlantic igneous province. *Earth and Planetary Science Letters* 201(2): 261–276.

Riisager P, *et al.* (2003) Paleomagnetic paleolatitude of Early Cretaceous Ontong Java Plateau basalts: Implications for Pacific apparent and true polar wander. *Earth and Planetary Science Letters* 208(3-4): 235–252.

Runcorn SK (1955) The Earth's magnetism. *Scientific American* 193(3): 152–154.

Runcorn SK (1956) Palaeomagnetic comparisons between Europe and North America. *Proceedings of the Geological Association of Canada* 8(1): 77–85.

Sabadini R (2002) Paleoclimate – Ice sheet collapse and sea level change. *Science* 295(5564): 2376–2377.
Sabadini R, *et al.* (1990) Eustatic sea level fluctuations induced by polar wander. *Nature* 345: 708–710.
Sabadini R, *et al.* (2002) Ice mass loss in Antarctica and stiff lower mantle viscosity inferred from the long wavelength time dependent gravity field. *Geophysical Research Letters* 29(10): 1373.
Sabadini R and Peltier WR (1981) Pleistocene deglaciation and the Earth's rotation – Implications for mantle viscosity. *Geophysical Journal of the Royal Astronomical Society* 66(3): 553–578.
Sager WW (2006) Cretaceous paleomagnetic apparent polar wander path for the pacific plate calculated from Deep Sea Drilling Project and Ocean Drilling Program basalt cores. *Physics of the Earth and Planetary Interiors* 156(3-4): 329–349.
Sager WW and Koppers AAP (2000a) Late Cretaceous polar wander of the Pacific plate: Evidence of a rapid true polar wander event. *Science* 287(5452): 455–459.
Sager WW and Koppers AAP (2000b) Late Cretaceous true polar wander: Not so fast. *Science* 288(5452): 2283a.
Satolli S, Besse J, Speranza F, and Calamita F (2007) The 125–150 Ma high-resolution Apparent Polar Wander Path for Adria from magnetostratigraphic sections in Umbria-Marche (Northern Apennines, Italy): Timing and duration of the global Jurassic–Cretaceous hairpin turn. *Earth and Planetary Science Letters* 257(1–2): 329–342.
Schmidt PW and Williams GE (1996) Palaeomagnetism of the ejecta-bearing Bunyeroo formation, Late Neoproterozoic, Adelaide fold belt, and the age of the Acraman impact. *Earth and Planetary Science Letters* 144(3-4): 347–357.
Schrag DP, *et al.* (2002) On the initiation of a snowball Earth. *Geochemistry Geophysics Geosystems* 3(6): (doi:10.1029/2001GC000219).
Schult FR and Gordon RG (1984) Root mean-square velocities of the continents with respect to the hot spots since the Early Jurassic. *Journal of Geophysical Research* 89(NB3): 1789–1800.
Seitz F and Schmidt M (2005) Atmospheric and oceanic contributions to Chandler wobble excitation determined by wavelet filtering. *Journal of Geophysical Research-Solid Earth* 110: B11406.
Sleep NH (1988) Gradual entrainment of a chemical layer at the base of the mantle by overlying convection. *Geophysical Journal-Oxford* 95(3): 437–447.
Soldati G, *et al.* (2001) The effect of global seismicity on the polar motion of a viscoelastic Earth. *Journal of Geophysical Research Solid Earth* 106(B4): 6761–6767.
Spada G (1997) Why are earthquakes nudging the pole towards 140 degrees E? *Geophysical Research Letters* 24(5): 539–542.
Spada G, *et al.* (2006) Glacial isostatic adjustment and relative sea-level changes: The role of lithospheric and upper mantle heterogeneities in a 3-D spherical Earth. *Geophysical Journal International* 165(2): 692–702.
Spada G and Boschi L (2006) Using the post-Widder formula to compute the Earth's viscoelastic Love numbers. *Geophysical Journal International* 166(1): 309–321.
Stacey F (1992) *Physics of the Earth*. 3rd edn. 513 pp. Brisbane, QLD: Brookfield Press.
Steinberger B and Oconnell RJ (1997) Changes of the Earth's rotation axis owing to advection of mantle density heterogeneities. *Nature* 387(6629): 169–173.
Steinberger B and O'Connell RJ (2002) The convective mantle flow signal in rates of true polar wander. In: Mitrovica JX and Vermeersen LLA (eds.) *Geodynamics Series 29: Ice Sheets, Sea Level and the Dynamic Earth*, pp. 233–256. Washington, DC: American Geophysical Union.
Stevenson DJ (1983) Planetary magnetic fields. *Reports on Progress in Physics* 46(5): 555–620.
Strik G, *et al.* (2003) Palaeomagnetism of flood basalts in the Pilbara Craton, western Australia: Late Archaean continental drift and the oldest known reversal of the geomagnetic field. *Journal of Geophysical Research-Solid Earth* 108(B12): 2551.
Tarduno JA, *et al.* (2003) The Emperor Seamounts: Southward motion of the Hawaiian hotspot plume in Earth's mantle. *Science* 301(5636): 1064–1069.
Tarduno JA and Cottrell RD (1997) Paleomagnetic evidence for motion of the Hawaiian hotspot during formation of the Emperor seamounts. *Earth and Planetary Science Letters* 153(3-4): 171–180.
Tarduno JA and Gee J (1995) Large-scale motion between Pacific and Atlantic hotspots. *Nature* 378(6556): 477–480.
Tarduno JA and Smirnov AV (2001) Stability of the Earth with respect to the spin axis for the last 130 million years. *Earth and Planetary Science Letters* 184(2): 549–553.
Tarduno JA and Smirnov AV (2002) Response to comment on 'Stability of the Earth with respect to the spin axis for the last 130 Million Years' by P. Camps, M. Prevot, M. Daignieres, and P. Machetel. *Earth and Planetary Science Letters* 198(3-4): 533–539.
Torsvik TH, *et al.* (1998) Polar wander and the Cambrian. *Science* 279: 9 (correction p. 307).
Torsvik TH, *et al.* (2002) Relative hotspot motions versus true polar wander. *Earth and Planetary Science Letters* 202(2): 185–200.
Tsai VC and Stevenson DJ (2007) Theoretical constraints on true polar wander. *Journal of Geophysical Research* 112: B05415 (doi:10.1029.2005JB003923).
Valeriano CM, *et al.* (2004) U–Pb geochronology of the southern Brasilia belt (SE-Brazil): Sedimentary provenance, Neoproterozoic orogeny and assembly of west Gondwana. *Precambrian Research* 130: 27–55.
Van der Voo R (1994) True polar wander during the Middle Paleozoic. *Earth and Planetary Science Letters* 122(1-2): 239–243.
Van Fossen MC and Kent DV (1992) Paleomagnetism of 122 Ma plutons in New England and the Mid-Cretaceous paleomagnetic field in North America: True polar wander or large-scale differential mantle motion? *Journal of Geophysical Research* 97: 19651–19661.
Veevers JJ (2004) Gondwanaland from 650–500 Ma assembly through 320 Ma merger in Pangea to 185–100 Ma breakup: Supercontinental tectonics via stratigraphy and radiometric dating. *Earth-Science Reviews* 68(1-2): 1–132.
Vermeersen LLA and Sabadini R (1999) Polar wander, sea-level variations and ice age cycles. *Surveys in Geophysics* 20(5): 415–440.
Ward PD, *et al.* (2005) Abrupt and gradual extinction among land vertebrates in the Karoo basin, South Africa. *Science* 307: 709–714.
Watts DR and Bramall AM (1981) Paleomagnetic evidence from the Ellsworth Mountains supports microplate nature of western Antarctica. *Geophysical Journal of the Royal Astronomical Society* 65(1): 271.
Wegener A (1929) *Die Entstehung der Kontinente und Ozeane. Vierte gaenzlich umgearbeitete Auflage*. Braunschweig, Germany: Druck and Verlag von Fridrich Vieweg und Sohn.
Zhong SJ and Hager BH (2003) Entrainment of a dense layer by thermal plumes. *Geophysical Journal International* 154(3): 666–676.
Zijderveld JD (1968) Natural remanent magnetizations of some intrusive rocks from Sor Rondane Mountains Queen Maud Land Antarctica. *Journal of Geophysical Research* 73(12): 3773–3785.

Raub et al., Figure 4

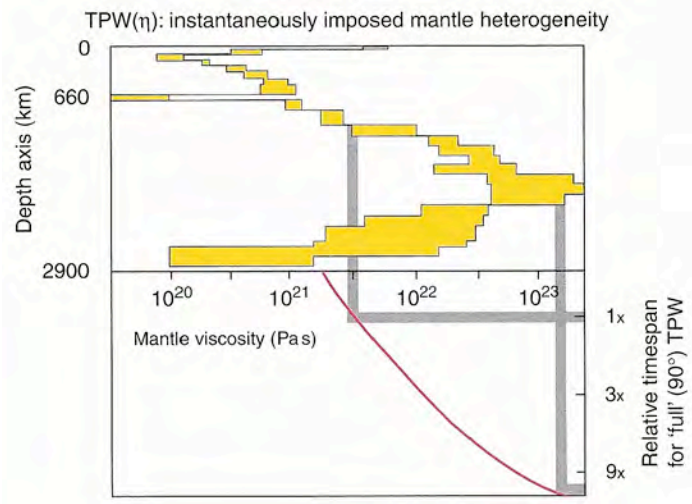

Raub et al., Figure 7

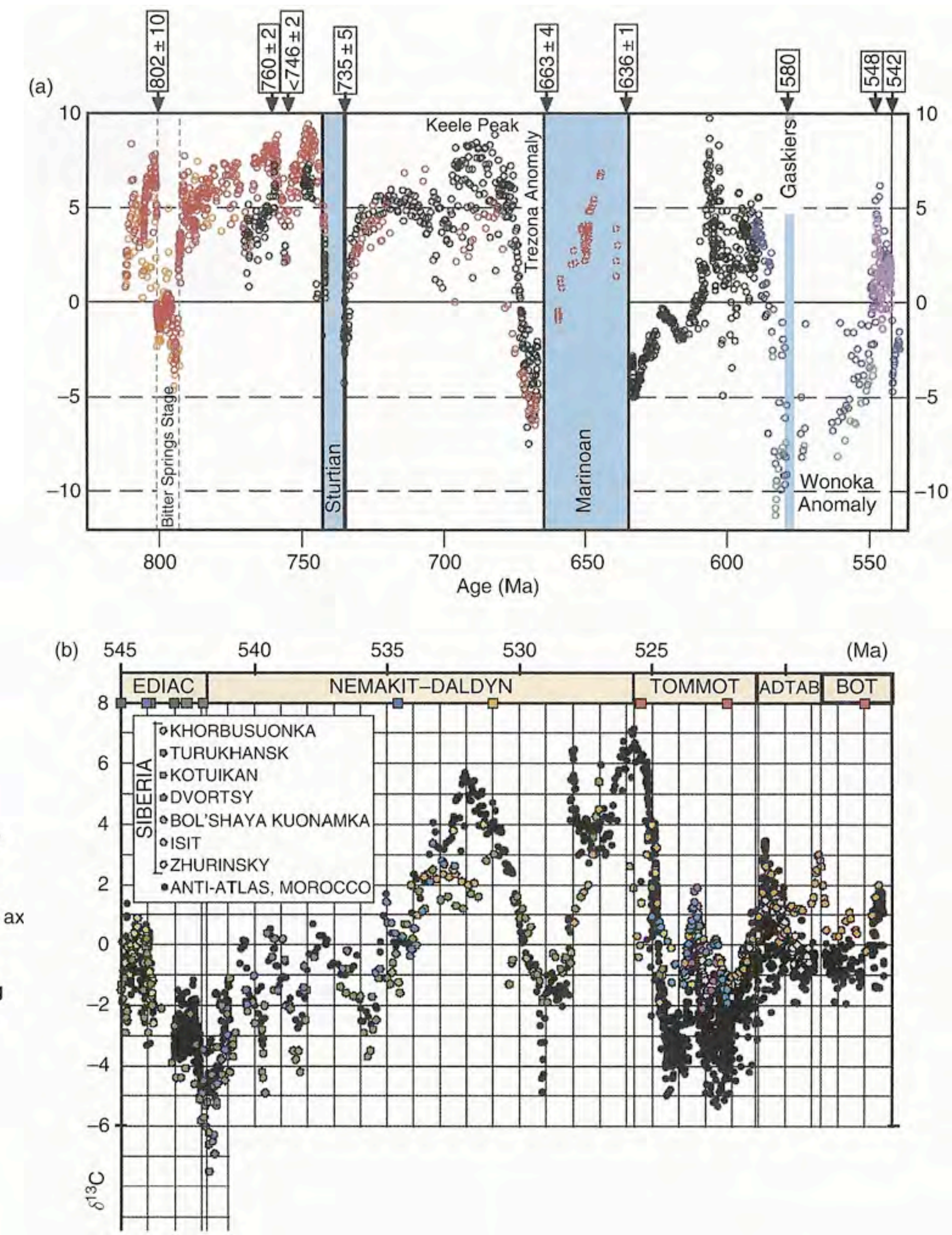

Raub et al., Figure 6

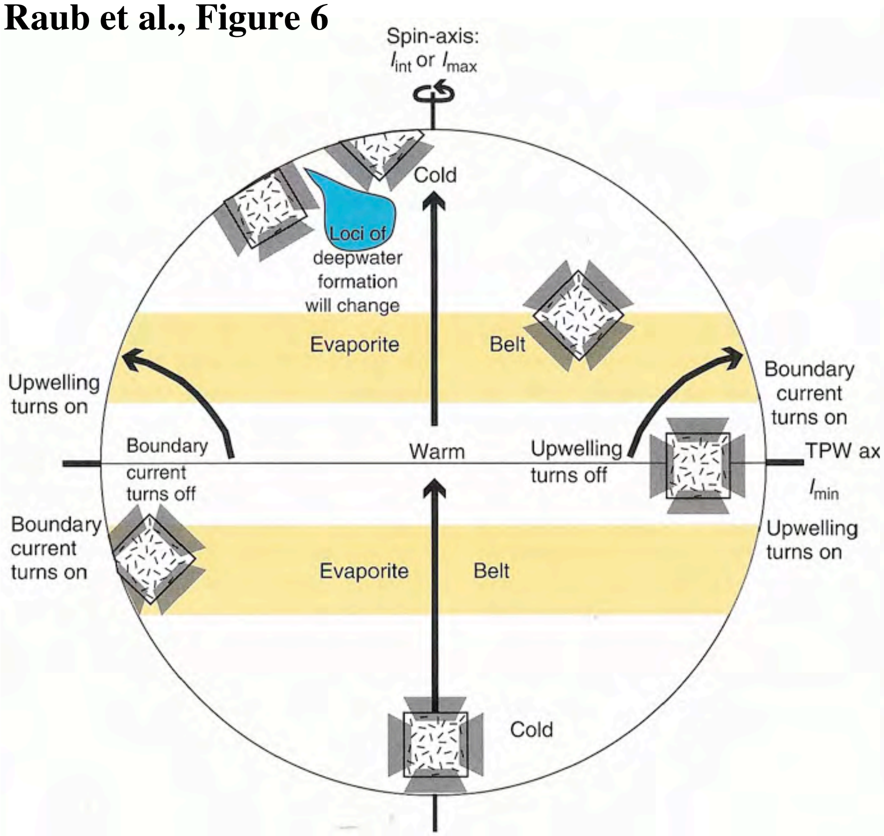

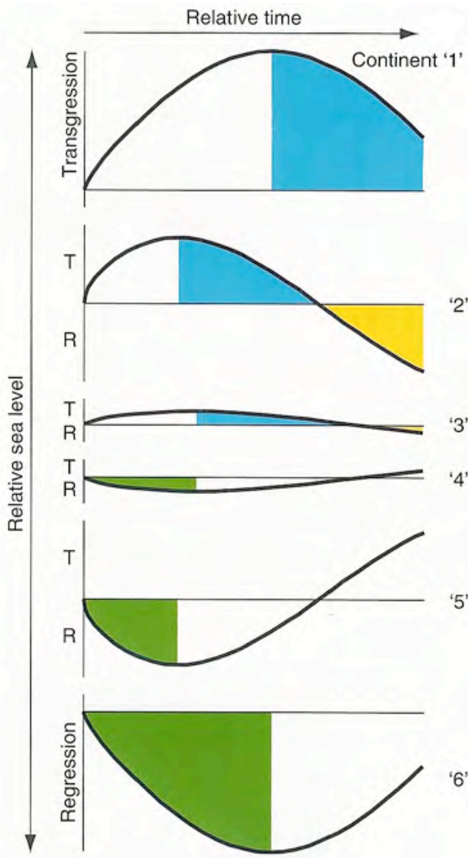

Raub et al.,
Figure 8

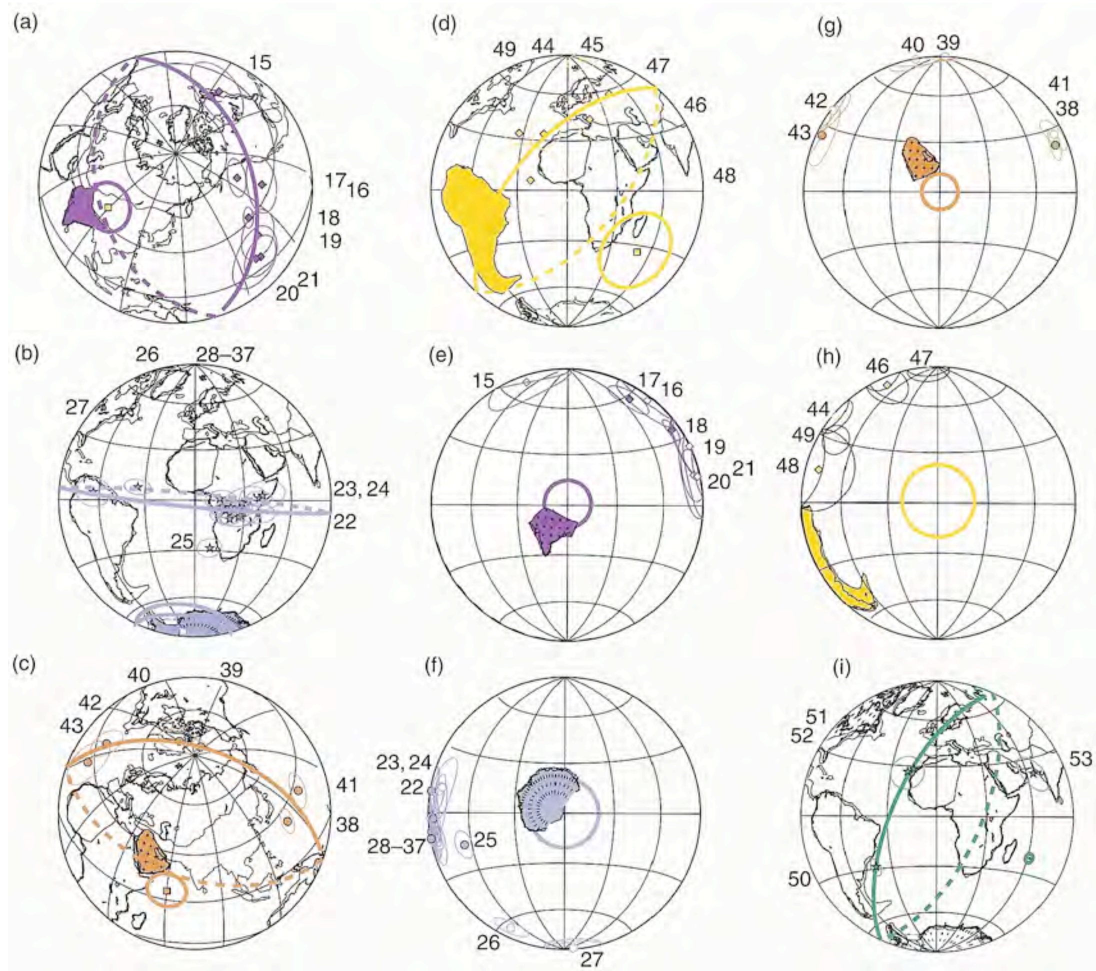

Raub et al.,
Figure 10

Raub et al., Figure 9

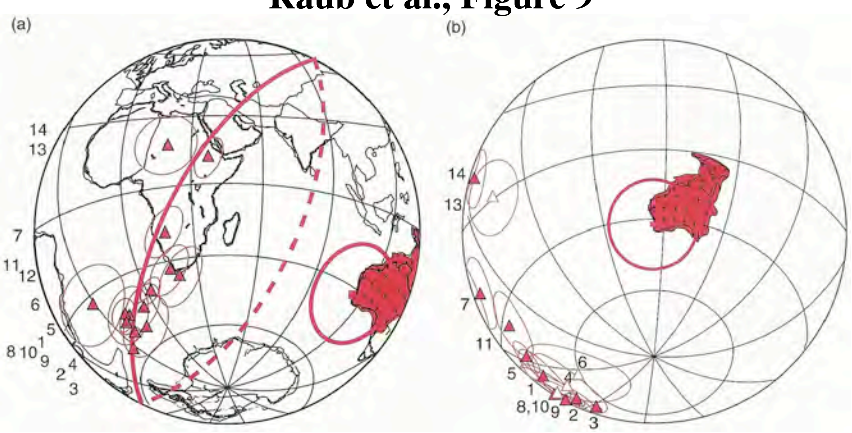

Raub et al., Figure 11